

Evaluation of dysplasias associated with inflammatory bowel disease

Zsófia Balajthy, MD

PhD Thesis

Szeged

2025

University of Szeged

Albert Szent-Györgyi Medical School

Doctoral School of Clinical Medicine

Evaluation of dysplasias associated with
inflammatory bowel disease

PhD Thesis

Zsófia Balajthy, MD

Supervisor: Anita Sejben MD, PhD

Szeged

2025

LIST OF PAPERS THAT SERVED AS THE BASIS OF THE PHD THESIS

I. Szintia Almási*, **Zsófia Balajthy***, Bence Baráth, Zsófia Krisztina Török, Panna Szaszák, Tamás Lantos, Bence Kővári, Anita Sejben: Examination of non-conventional dysplasias adjacent to colorectal adenocarcinoma in patients with IBD. Pathol Oncol Res. 2025; 3:30:1611978. doi: 10.3389/pore.2024.1611978

Q2; IF (2024): 2.3

(*contributed equally)

II. **Zsófia Balajthy**, Panna Szaszák, Szintia Almási, Tamás Lantos, Anita Sejben: Evaluation of dysplasias associated with inflammatory bowel disease – a single-center, retrospective, 5-year experience. Pathol Oncol Res. 2025; 15:31:1612105. doi: 10.3389/pore.2025.1612105

Q2; IF (2024): 2.3

III. **Zsófia Balajthy**, Szintia Almási, Tamás Lantos, Levente Kuthi, Georgios Deftereos, Won-Tak Choi, Anita Sejben: Whole-exome sequencing analysis of inflammatory bowel disease-associated serrated dysplasia. Pathol Oncol Res. 2025; 26:5704. doi: 10.3390/ijms26125704

Q1; IF (2024): 4.9

OTHER PUBLICATIONS

IV. Roland Fejes, Kitti Szonja Gyorgyev, Csaba Góg, László Krenács, Tamás Zombori, Zsófia Eszter Széll, **Zsófia Balajthy**, Tamás Pancsa and Zsolt Simonka: World J Surg Oncol. 2024; 22:299. doi: 10.1186/s12957-024-03563-7

Q1; IF (2024): 2.5

V. Roland Fejes*, **Zsófia Balajthy***, Csaba Góg, Ágota Vajda, Fanni Hegedűs, Zsolt Simonka, Szabolcs Ábrahám: Colonic endometriosis: from subtotal bowel obstruction to malignant transformation - a case series and literature review. World J Surg Oncol. 2025; 23:230. doi: 10.1186/s12957-025-03888-x

Q1; IF (2024): 2.5

(*contributed equally)

TABLE OF CONTENTS

LIST OF ABBREVIATIONS	II.
LIST OF FIGURES	IV.
LIST OF TABLES	IV.
1. INTRODUCTION	1.
1.1. Non-conventional dysplasias associated with inflammatory bowel disease	1.
1.2. IBD-associated serrated dysplasias	3.
2. AIMS	5.
3. MATERIALS AND METHODS	5.
3.1. Examination of NCDs adjacent to colorectal adenocarcinoma in patients with IBD	5.
3.2. Evaluation of dysplasias associated with IBD – a single-center, retrospective, 5-year experience	6.
3.3. WES analysis of IBD-associated serrated dysplasia	6.
4. RESULTS	9.
4.1. Examination of NCDs adjacent to colorectal adenocarcinoma in patients with IBD	9.
4.1.A. Patients' epidemiological and clinical data	9.
4.1.B. Histopathological evaluation and IBD-associated neoplasia	11.
4.2. Evaluation of dysplasias associated with IBD – a single-center, retrospective, 5-year experience	13.
4.2.A. General clinicopathologic characteristics	13.
4.2.B. Clinicopathologic characteristics of IBD-associated conventional dysplasias	13.
4.2.C. Evaluation of IBD-associated adenocarcinomas in patients with conventional dysplasia	15.
4.2.D. Clinicopathologic characteristics of IBD-associated NCD	16.
4.2.E. Evaluation of IBD-associated adenocarcinomas in patients with NCD	18.
4.2.F. Clinicopathologic characteristics of IBD-associated, combined conventional dysplasia and NCD	19.
4.2.G. Evaluation of IBD-associated adenocarcinomas in patients with combined conventional dysplasias and NCD	19.
4.2.H. Survival analysis	20.
4.3. WES analysis of IBD-associated serrated dysplasia	22.
4.3.A. Clinicopathologic features of serrated dysplasia	22.
4.3.B. Molecular features of serrated dysplasia	25.
5. DISCUSSION	27.
5.1. Examination of NCDs adjacent to colorectal adenocarcinoma in patients with IBD	27.
5.2. Evaluation of dysplasias associated with IBD – a single-center, retrospective, 5-year experience	36.
5.3. WES analysis of IBD-associated serrated dysplasia	39.
6. CONCLUSIONS	42.
7. ACKNOWLEDGEMENT	43.
8. REFERENCES	44.

LIST OF ABBREVIATIONS

ACVR2A - Activin A receptor type 2A

ASXL1 - Additional sex combs like 1

ATR - Ataxia telangiectasia and rad3-related

BRAF - v-Raf murine sarcoma viral oncogene homolog B

CCD - Crypt cell dysplasia

CD - Crohn's disease

CDC6 - Cell division cycle 6

CDKN1b - Cyclin-dependent kinase inhibitor 1B

CDX2 - Caudal-type homeobox transcription factor 2

CK7 - Cytokeratin 7

CK20 - Cytokeratin 20

CRC - Colorectal cancer

DFS - Disease-free survival

DNA - Deoxyribonucleic acid

DPD - Dysplasia with increased Paneth cell differentiation

EXT1 - Exostosin glycosyltransferase 1

GCD - Goblet cell-deficient dysplasia

HE - Hematoxylin and eosin

HIF1A - Hypoxia-inducible factor 1-alpha

IBD - Inflammatory bowel disease

IDH1 - Isocitrate dehydrogenase 1

ICD - International Classification of Diseases

KMT2C - Lysine N-methyltransferase 2C

KRAS - Kirsten rat sarcoma virus

MADD - MAP kinase-activating death domain

MAPK - Mitogen activated protein kinase

MASPIN - Mammary serine protease inhibitor

MAX - MYC-associated factor X

MGA - MAX dimerization protein MGA

MGMT - O(6)-Methylguanine-DNA-methyltransferase

MLH1 - MutL homolog 1

MMR - Mismatch repair

MPL - Myeloproliferative leukaemia virus gene

MSH2 - MutS homolog 2

MSH6 - MutS homolog 6

MSI - Microsatellite instability

MUC2 - Mucin 2

MUC5AC - Mucin-5AC

MUC6 - Mucin 6

MUTYH - MutY DNA glycosylase

NA - Not applicable

NCD - Non-conventional dysplasia

NOS - Not otherwise specified	SERPINB4 - Serine proteinase inhibitor, clade B
NRAS - Neuroblastoma ras viral oncogene homolog	SETD1B - SET domain containing 1B
OS - Overall survival	SOX9 - SRY-box transcription factor 9
PMS2 - PMS1 homolog 2	SSL - Sessile serrated lesion
POLE - Polymerase epsilon	TGFBR2 - Transforming growth factor beta receptor 2
p53 - Tumour protein p53	TNM - Tumour, Node, Metastasis
PFS - Progression-free survival	TSC1 - Tuberous sclerosis 1
POLG - DNA polymerase subunit gamma	TSA - Traditional serrated adenoma
PSC - Primary sclerosing cholangitis	UC - Ulcerative colitis
PTEN - Phosphatase and ten sin homolog	WES - Whole exome sequencing
SEC - Serrated epithelial change	ZNF292 - Zinc finger protein 292

LIST OF FIGURES

FIGURE 1. Serrated dysplastic subtypes.	7.
FIGURE 2. Kaplan-Meier curves of conventional and NCDs	11.
FIGURE 3. Microscopic features of IBD-associated NCDs of the examined population.....	12.
FIGURE 4. Microscopic features of IBD-associated, conventional dysplasias	14.
FIGURE 5. Microscopic features of IBD-associated, NCDs	18.
FIGURE 6. Kaplan-Meier estimates of PFS and OS in patients with conventional dysplasia	21.
FIGURE 7. Kaplan-Meier estimates of PFS and OS in patients with NCD.....	21.
FIGURE 8. Kaplan-Meier estimates of PFS and OS in patients with combined conventional and NCD	21.
FIGURE 9. Immunohistochemical analysis of SSL-like dysplasia and serrated dysplasia, NOS	26.

LIST OT TABLES

TABLE 1. Epidemiological and clinicopathologic characteristics of the included cohort.....	10.
TABLE 2. Clinicopathological characteristics of the identified conventional dysplasias	15.
TABLE 3. Clinicopathological characteristics of the identified NCDs	17.
TABLE 4. Clinicopathologic features of the IBD patients with serrated dysplasia	22.
TABLE 5. Clinicopathologic features of the serrated dysplastic subtypes.....	24.
TABLE 6. Molecular features of serrated dysplasia.....	26.
TABLE 7. Results of the literature review	29.

1. INTRODUCTION

1.1. Non-conventional dysplasias associated with inflammatory bowel disease

Inflammatory bowel disease (IBD) encompasses a group of chronic, relapsing inflammatory disorders of the gastrointestinal tract, primarily including Crohn's disease (CD), ulcerative colitis (UC), and indeterminate colitis. These diseases are characterized by alternating periods of flare-ups and remission, significantly impairing patients' quality of life and often requiring continuous medical supervision. While the exact cause of IBD remains incompletely understood, a complex interplay of genetic predisposition, environmental triggers, gut microbiota imbalance, and immune dysregulation is believed to underlie disease onset and progression. Among these entities, CD can affect any segment of the gastrointestinal tract from the oral cavity to the anus, but it most frequently involves the terminal ileum, often manifesting with transmural inflammation, strictures, or fistula formation [1, 2]. In contrast, UC is limited to the mucosal layer of the colon and rectum, with inflammation that may remain confined to the rectum or extend proximally to involve the entire colon. Cases that exhibit overlapping clinical, endoscopic, and histopathological features of both UC and CD but cannot be precisely classified are designated as indeterminate colitis [3].

Due to the chronic, relapsing nature of IBD, patients accumulate a substantial inflammatory burden over time, which, when combined with alterations in the intestinal microbiome and aberrant immune responses, predisposes them to the development of neoplastic changes in the colorectal mucosa [4, 5]. Epidemiological studies have shown that IBD patients face approximately a twofold higher risk of developing colorectal neoplasia compared with the general population, largely due to the pro-tumorigenic effects of persistent inflammation [2]. The risk of neoplastic transformation is influenced by several clinical parameters, including early age of IBD onset, disease duration and severity, cumulative inflammatory activity, frequency of relapses, presence of inflammatory pseudopolyps, coexistent primary sclerosing cholangitis (PSC), and family history of colorectal cancer (CRC). From a molecular standpoint, many signaling pathways implicated in IBD overlap with those involved in colorectal carcinogenesis - such as those regulating cell proliferation, apoptosis, angiogenesis, and chronic inflammation - though certain mechanistic distinctions remain [6].

Historically, therapeutic strategies for IBD were largely directed toward symptomatic relief and suppression of acute inflammation. However, in recent years, the focus has shifted toward achieving deep remission, mucosal healing, and prevention of long-term complications such as dysplasia, CRC, and disease-related hospitalizations [7]. Although most advanced therapies,

including biologics and small-molecule inhibitors, primarily target inflammatory pathways, they have contributed to a notable reduction in the incidence of IBD-associated neoplasia [8]. The integration of regular endoscopic surveillance, improved imaging techniques, and advances in endoscopic resection has further decreased the risk of dysplasia and CRC among IBD patients over the past few decades [9-11].

According to contemporary guidelines, screening for colorectal carcinoma in IBD should commence approximately 8 years after the initial diagnosis [5, 11]. Current management approaches are stratified based on whether dysplastic lesions are visible endoscopically or detected only in random biopsies. For visible or polypoid lesions, therapeutic decisions - ranging from endoscopic resection to surveillance colonoscopy - depend on the completeness of lesion excision. In contrast, for lesions identified in random biopsies, low-grade dysplasia may warrant close endoscopic surveillance or, in certain cases, surgical colectomy, whereas high-grade dysplasia generally necessitates colectomy due to the high likelihood of concurrent or imminent carcinoma [6].

Traditionally, histological assessment of dysplasia in IBD relied on the Riddell classification system [12]. However, beyond conventional dysplasia and CRC, IBD patients are susceptible to developing non-conventional dysplasia (NCD) subtypes with distinct morphological and molecular characteristics. Choi et al. described several categories of NCD, including hypermucinous dysplasia, dysplasia with increased Paneth cell differentiation (DPD), goblet cell-deficient (GCD) dysplasia, crypt cell dysplasia (CCD), traditional serrated adenoma (TSA)-like, sessile serrated lesion (SSL)-like, and serrated dysplasia not otherwise specified (NOS) [13].

Hypermucinous dysplasia is typified by tubulovillous or villous architecture with prominent mucinous differentiation involving more than 50% of the lesion. DPD, in contrast, displays tubular crypts lined by elongated, hyperchromatic nuclei and increased Paneth cell differentiation, with at least 2 contiguous crypts exhibiting this feature across separate foci. GCD is characterized by a near-complete absence of goblet cells within dysplastic crypts, distinguishing it from DPD. To ensure accurate differentiation between true dysplasia and reactive epithelial changes, the presence of unequivocal cytologic or architectural atypia - such as loss of surface maturation - is essential. Both DPD and GCD are generally categorized as intestinal-type NCDs. CCD is morphologically characterised by round-to-oval, nonstratified nuclei, and Paneth cell differentiation is solely occasionally visible [13]. The morphological details of the remaining NCD variants are discussed in Chapter 1.2.

Although most NCDs display low-grade histological features, accumulating evidence, particularly from North American cohorts, indicates that they may carry a less favorable prognosis. NCDs are more frequently associated with genomic instability, including aneuploidy, and are often linked to advanced neoplasia such as poorly differentiated and signet ring cell carcinomas. Furthermore, several subtypes - particularly hypermucinous, GCD, and CCD - tend to present as flat or even endoscopically invisible lesions, complicating their detection and necessitating more extensive biopsy protocols and random sampling during surveillance colonoscopies [13-15]. These lesions commonly arise in the same anatomic regions where colorectal carcinomas develop, supporting their potential role as precursor lesions [16]. They have also been associated with emerging histologic variants of IBD-related colorectal carcinoma, including tubuloglandular, GCD, and serrated phenotypes [11, 17]. Current data suggest that NCDs may be present in approximately one-quarter to one-half of IBD-associated colorectal adenocarcinomas [13]. Nevertheless, given the relative novelty of these classifications and the limited number of comprehensive studies, both the clinical implications and diagnostic recognition of NCDs remain challenging areas requiring further investigation.

1.2. IBD-associated serrated dysplasias

Among the spectrum of non-conventional dysplasias associated with inflammatory bowel disease (IBD), three distinct serrated subtypes with dysplasia - collectively referred to as serrated dysplasia - have been recognized. These include SSL-like dysplasia, TSA-like dysplasia, and serrated dysplasia, NOS. These subtypes exhibit morphological and molecular features reminiscent of their sporadic counterparts but arise within a background of chronic mucosal inflammation, architectural distortion, and regenerative changes typical of IBD, making their recognition particularly challenging in routine diagnostic practice [6, 13, 14, 17-27]. SSL-like dysplasia is characterized by architectural features resembling those seen in sporadic sessile serrated lesions, particularly the presence of dilated, L-shaped, or inverted T-shaped crypts extending toward or abutting the muscularis mucosae. These distorted crypts often display serrated epithelial infoldings and are lined by dysplastic epithelium demonstrating nuclear enlargement, hyperchromasia, and loss of polarity. The overall architecture tends to be flat or slightly elevated, and endoscopically these lesions may be subtle or even invisible, emphasizing the importance of histological recognition in biopsy material. TSA-like dysplasia, by contrast, typically displays a tubulovillous or villous architecture with prominent slit-like serrations and ectopic crypt formation. The lining epithelium is composed

of elongated, stratified columnar cells with eosinophilic cytoplasm and pencillate nuclei, closely resembling the morphology of sporadic traditional serrated adenomas. The dysplastic process is often low-grade, though foci of high-grade atypia may occasionally occur. These lesions tend to arise in the distal or left colon, paralleling the anatomical distribution of sporadic TSAs [14, 19, 20]. The third serrated subtype, serrated dysplasia, NOS, encompasses lesions demonstrating a complex serrated glandular architecture with unequivocal cytologic dysplasia that does not fully satisfy the diagnostic criteria for SSL-like or TSA-like dysplasia. The serrations in these lesions may be irregular or disorganized, and the degree of cytological atypia can vary widely. Although the clinicopathologic and molecular characteristics of serrated dysplasia, NOS remain poorly defined, its recognition as a distinct category reflects the heterogeneity of serrated lesions arising in the context of chronic colitis [14, 26].

From a molecular perspective, emerging evidence suggests that IBD-associated serrated dysplasias may share several key genetic alterations with their sporadic counterparts, supporting a possible convergence of serrated neoplastic pathways across etiologic contexts. For instance, SSL-like dysplasia is more commonly found in the right colon, consistent with the distribution of sporadic SSLs, while TSA-like dysplasia predominates in the left colon, mirroring sporadic TSAs [14, 19, 20]. Furthermore, low-grade serrated dysplasia in IBD frequently harbors *KRAS* mutations (approximately 45%) and, less commonly, *BRAF* mutations (approximately 18%) - a pattern comparable to that observed in sporadic TSA cases [19]. These findings suggest that the serrated pathway of carcinogenesis, typically defined by aberrant MAPK signaling, may also operate in the setting of IBD, albeit within a distinct inflammatory microenvironment.

Despite these intriguing parallels, the true clinical and biological significance of serrated dysplasia in IBD remains insufficiently understood. This is largely due to its low prevalence, with each serrated dysplastic subtype estimated to represent only about 1% of all IBD-associated dysplastic lesions, resulting in limited case series and inconsistent diagnostic criteria across studies. Consequently, the full spectrum of histological variability, molecular alterations, and progression risk to carcinoma remains incompletely characterized [13, 18, 22]. Nevertheless, accumulating data suggest that recognition of these serrated patterns is critical, as they may define a subset of IBD-associated neoplasia with distinct morphologic evolution, molecular drivers, and potentially unique clinical behavior. Continued efforts to standardize diagnostic terminology and integrate molecular findings are therefore essential to advance our understanding of serrated neoplasia within the IBD landscape.

2. AIMS

The aims of the thesis are as follows:

1. To re-evaluate a cohort of IBD-associated adenocarcinoma cases, retrospectively identify associated NCDs and validate recent North American findings in a Central-Eastern European population, and to provide an updated literature review.
2. To identify of IBD-associated NCDs within a consecutive single-center study, as well as to evaluate clinicopathological parameters influencing the prognosis of NCDs.
3. To further characterize serrated dysplasias and investigate their molecular features via whole-exome sequencing (WES).

3. MATERIALS AND METHODS

3.1. Examination of NCDs adjacent to colorectal adenocarcinoma in patients with IBD

A series of 28 randomly chosen cases of known IBD associated colorectal adenocarcinomas, diagnosed between 2010 and 2022, at the Department of Pathology, University of Szeged was included. In all cases, the patient's gender, age both at the diagnosis of IBD and neoplasia, type and localisation of IBD, type of specimen [biopsy (n = 8) / surgical specimens (n = 20)], as well as the histological type, grade, localisation, and stage of cancer, disease-free (DFS) and overall survival (OS) were obtained by chart review. Furthermore, all the patients' prior gastrointestinal histology reports have been reviewed and mean histologic activity of IBD in a 5-year interval before the neoplastic sample was registered. The patients' index cases yielding the adenocarcinoma diagnosis were independently re-evaluated by 2 gastrointestinal pathologists (Bence Péter Kővári, Anita Sejben), focusing on identifying conventional and NCDs as candidate precursor lesions adjacent to the adenocarcinoma. If present, NCD was subclassified as hypermucinous, DPD, GCD, CCD, TSA-like, SSL-like, and serrated dysplasia, NOS following the morphologic criteria published by Choi et al [13, 26]. Subsequently, discrepant interpretations were revisited using a multiheaded microscope and discussed to achieve consensus. Statistical analyses were carried out by the R statistical software (v4.1.1). The Mann Whitney test was used to compare two groups of independent samples (from non-normally distributed data). The association between categorical variables was examined by Fisher's exact test (with Bonferroni-Holm correction). The Kaplan-Meier method was used to estimate

DFS/OS curves, and the logrank test was applied to compare survival curves. All statistical tests were two sided, and p-values of less than 0.05 were considered statistically significant. Kaplan-Meier curves were created using the R package “survminer” (v0.4.9). This study was approved by the institutional ethical committee of the Albert Szent-Györgyi Clinical Centre of the University of Szeged (107/2021-SZTE/ RKEB; 4988).

3.2. Evaluation of dysplasias associated with IBD – a single-center, retrospective, 5-year experience

All IBD patients diagnosed at the Department of Pathology, University of Szeged, Hungary, between 2011 and 2015 were identified based on ICD codes, and neoplastic samples from these patients were subsequently reviewed. During database construction, clinicopathological characteristics including the age, sex, type, duration, and localization of IBD were collected. The histological type, date of diagnosis, lesion size, and morphology observed during endoscopy were retrospectively documented in the case of dysplastic samples. In cases of invasive tumors, additional data including histological type, date of tumor diagnosis, grade, macroscopic morphology, localization, TNM stage, and the presence of vascular or lymphatic invasion. Progression-free survival (PFS) was solely defined in those cases who developed colorectal carcinoma during follow-up, while OS was defined in all cases. Histological evaluation was utilized with an Olympus BX53F microscope. A diagnosis of NCD was established only when the observed lesion was present in at least 50% of the sample. If multiple types of NCDs were observed within a single slide, a dominant pattern was selected, based on the extent and size of the lesions for statistical analysis. This study does not address multiplex lesions; however, our research group plans to focus on this aspect in future investigations. Statistical analyses were performed using Fisher’s exact test and chi-square test for discrete variables, as well as the Mann–Whitney U test and two-sample t-test for continuous variables. $P < 0.05$ was considered statistically significant. Our study was approved by the Medical Research Council (BM/28834-1/2024).

3.3. WES analysis of IBD-associated serrated dysplasia

We retrospectively reviewed data from 2396 patients treated for UC ($n = 1400$), CD ($n = 970$), and indeterminate colitis ($n = 26$) at the University of Szeged between 2011 and 2023. Among them, 177 (7%) patients were diagnosed with colorectal neoplasia, of which only 11 (6%) had serrated dysplasia ($n = 13$) (Figure 1).

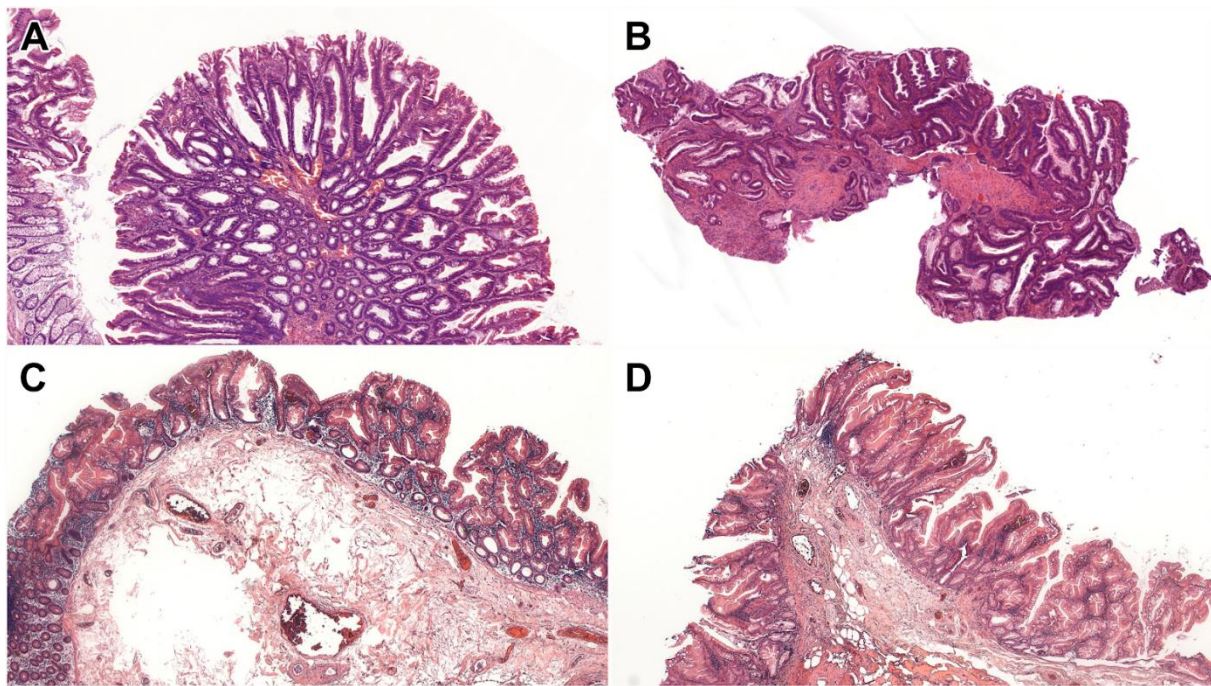


Figure 1 Serrated dysplastic subtypes. (A) SSL-like dysplasia shows dilated crypts at the interface with the muscularis mucosae, accompanied by dysplastic epithelium (HE, 5x). (B) Serrated dysplasia, NOS demonstrates a complex serrated architecture with dysplasia. There is no definite evidence of SSL-like dysplasia or TSA-like dysplasia (HE, 5x). (C, D) In mixed SSL-like/TSA-like dysplasia, one area shows SSL-like dysplasia characterized by dilated L-shaped or inverted T-shaped crypts at the interface with the muscularis mucosae (C; HE, 5x), while another area shows TSA-like dysplasia featuring a tubulovillous growth pattern, eosinophilic cytoplasm, and slit-like serrations (D; HE, 5x). Abbreviation: HE - Hematoxylin and eosin.

All serrated dysplastic lesions were reevaluated and subtyped regardless of the sample type (biopsy/resection) by 2 gastrointestinal pathologists (Won-Tak Choi and Anita Sejbén) based on the published morphologic criteria [6, 13, 14, 17, 18, 24-26]. For each patient, relevant clinicopathologic information was also collected by reviewing their medical charts and pathology reports. This included age, gender, IBD characteristics (such as subtype, extent, and duration), presence of PSC, and features of dysplasia (including location, endoscopic appearance, size, and histologic grade). Additionally, data on any concurrent or subsequent dysplasia and CRC were collected. PFS was defined either as dysplasia recurrence or carcinoma development in the same colon segment, while OS was calculated until the end of follow-up or death. Regarding WES, 10 serial sections, each 10 µm thick, were cut from the paraffin block for each sample. Deparaffinization and Proteinase K treatment were performed overnight at 55 °C. The extracted DNA was purified using the 0.5 vol KAPA Pure Bead (Roche, Mannheim, Germany) and eluted in 20 µL of 10 mM Tris-HCl pH 8 buffer. The DNA concentration was determined using the Quant-iT 1x dsDNA HS Assay kit (Thermo Fisher Scientific, Waltham, MA, USA) and measured with a Fluostar Omega (BMG Labtech, Ortenberg, Germany; Software version: 1.01) plate reader. For the library construction, the Twist Library Preparation

EFKit 2.0 with the Universal Adaptor System and Exome 2.0 Panel (Twist Bioscience, South San Francisco, CA, USA) was used, following the manufacturer's protocol. The fragment size distribution of the pre-capture and post-capture libraries was determined using capillary electrophoresis on the LabChip GX Touch HT Nucleic Acid Analyzer, employing the X-Mark HTChip and the DNA NGS 3K Assay kit (PerkinElmer, Waltham, MA, USA). The libraries were quantified using the Quant-iT 1x dsDNA HS Assay kit (Thermo Fisher Scientific, Waltham, MA, USA) with Fluostar Omega (BMG Labtech, Ortenberg, Germany). The pooled libraries were diluted to 1.5 nM and prepared for 2×150 bp paired-end sequencing using the 300-cycle S4 Reagent Kit on the NovaSeq 6000 Sequencing System (Illumina, San Diego, CA, USA), following the manufacturer's protocol. On average, more than 24 Gbp of raw data was generated per sample. Demultiplexing, adapter trimming, Q30-filtering, and somatic variant calling of the sequenced data were performed on the Dragen Bio-IT platform (Illumina, San Diego, CA, USA). Genomic variants of Vcf files were annotated using the Nirvana Software package (OncoKB Database) [28]. Variants were manually reviewed for the read quality and the number of reads. The variants had to show at least 10 variant reads to be considered for further analysis. Pathogenic and likely pathogenic reads in genes with known oncogenic or tumor suppressor activity were included in the results (ClinVar Database) [29]. Also, variants that resulted in a frameshift, non-sense (stop-gain), splice donor/splice acceptor site altering, or transcription start site altering in the tumor suppressor genes (OncoKB Database) were included [28].

4. RESULTS

4.1. Examination of NCDs adjacent to colorectal adenocarcinoma in patients with IBD

4.1.A. Patients' epidemiological and clinical data

The demographic and clinicopathologic characteristics of the included cases are shown in Table 1. The mean age at carcinoma diagnosis was 47 years in the exclusively conventional and 50 years in the NCD group. Definite male predominance was found in the examined, IBD associated adenocarcinoma population in general (male-to female ratio 22:6). The male-to-female ratios in the exclusively conventional and NCD groups were 10:1 and 6:2, respectively, which reflects the clear male predominance in both subpopulations. All examined patients were Caucasians. In all groups, the majority of patients suffered from UC. The average duration of IBD at the time of carcinoma diagnosis was 16 years (range: 0–50 years, median: 14). Previous histological samples and reports were not available in 8 cases. Active disease was defined in 12 patients with UC, and 5 CD patients. Active disease was not present in 3 patients. In the exclusively conventional dysplasia group (n = 11), 8 patients were diagnosed with UC, while in the exclusively NCD group (n = 8), the number of patients was 7, and in the mixed group (n = 9), it proved to be 5. Patients with UC developed adenocarcinoma localised to the colon segment previously reported to be involved by inflammation; in the left (11/20; 55%) and in the right colon (9/20; 45%), while 12.5% (1/8) and 87.5% (7/8) of patients with CD presented with right-sided and left-sided colon cancer, respectively.

	Conventional dysplasia exclusively (n=11)	NCD exclusively (n=8)	Mixed conventional and NCD cases (n=9)	p-values
Average age (at the time of carcinoma diagnosis)	47	50	49	At last follow-up – $p=0.218$; at the diagnosis of IBD – $p=0.275$; at malignant diagnosis – $p=0.170$
Male:female ratio	10:1	6:2	6:3	$p=0.524$
Type of IBD	CD: 3 UC: 8	CD: 1 UC: 7	CD: 4 UC: 5	$p=0.223$
Average duration of IBD	16.1 years (range: 1-50)	15.8 years (range: 0-27)	16.2 years (range: 0-21)	$p=0.926$
Activity of IBD				
Histological subtype of associated colorectal adenocarcinoma	Conventional adenocarcinomas: 8 Medullary adenocarcinomas: 3	Conventional adenocarcinomas: 4 Mucinous adenocarcinomas: 4	Conventional adenocarcinomas: 9	$p=0.014$ and $p=0.041$
Grade of associated colorectal adenocarcinoma	1: 2 2: 7 3: 2	2: 5 3: 3	1: 1 2: 5 3: 3	$p=0.093$
Stage of associated colorectal adenocarcinoma	T1: 1 T3: 7 T4: 3	T2: 1 T3: 3 T4: 4	T3: 7 T4: 2	$p=0.131$
Location of associated colorectal adenocarcinoma	Left colon: 6 Right colon: 5	Left colon: 3 Right colon: 5	Left colon: 4 Right colon: 5	$p=0.253$

Table 1 Epidemiological and clinicopathologic characteristics of the included cohort.

From the examined population, only 2 patients were noted to have PSC; 1 belonged to the conventional dysplasia group, while the other had NCD. Family history was negative for polyposis syndromes in all cases. With statistical analysis, there was no significant association found between NCD and gender ($p = 0.524$), age (at last follow-up – $p = 0.218$; at the diagnosis of IBD – $p = 0.275$; at malignant diagnosis – $p = 0.170$), type of IBD ($p = 0.223$), duration of IBD ($p = 0.926$), and disease activity ($p = 1$). For DFS, the 2 groups (i.e., patients with conventional and NCD) had very similar survival curves ($p = 0.900$) (Figure 2A). The differences were also not significant ($p = 0.257$) for the OS (Figure 2B). The Kaplan-Meier curves are displayed in Figure 2.

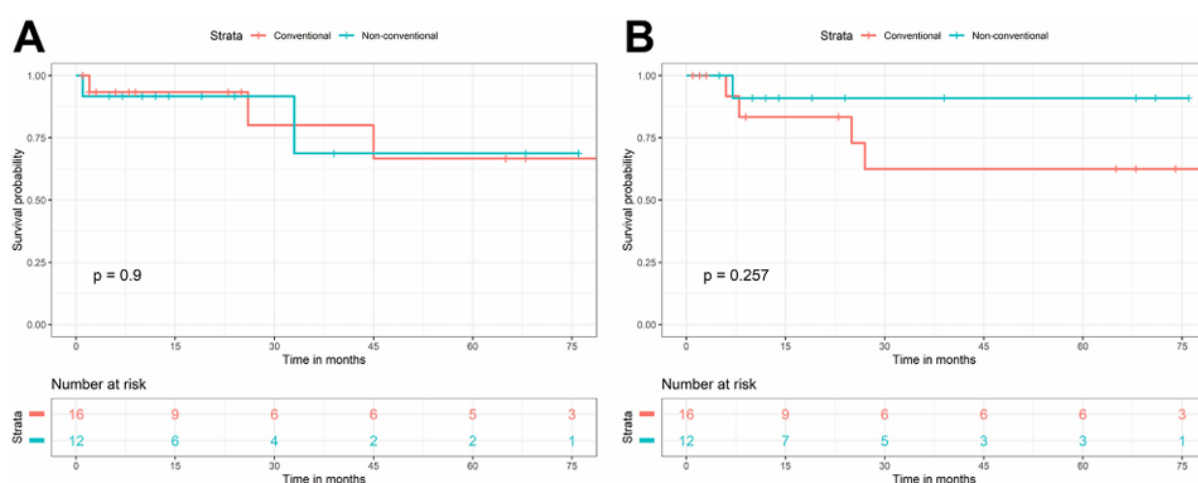


Figure 2 Kaplan-Meier curves of conventional and NCDs, regarding DFS (A) and OS (B).

4.1.B. Histopathological evaluation and IBD associated neoplasia

Adjacent to the previously reported adenocarcinomas, exclusively conventional dysplasia was detected in 11, while exclusively NCD in 8 patients. Dysplasia comprised of a combination of conventional and at least one subtype of NCD was observed in 9 patients. Altogether, 25 NCD foci were identified, including hypermucinous (n = 9) (Figure 3A), GCD (n=6) (Figure 3B), serrated dysplasia, NOS (n=6) (Figure 3C), and TSA-like dysplasia (n = 4) (Figure 3D) subtypes.

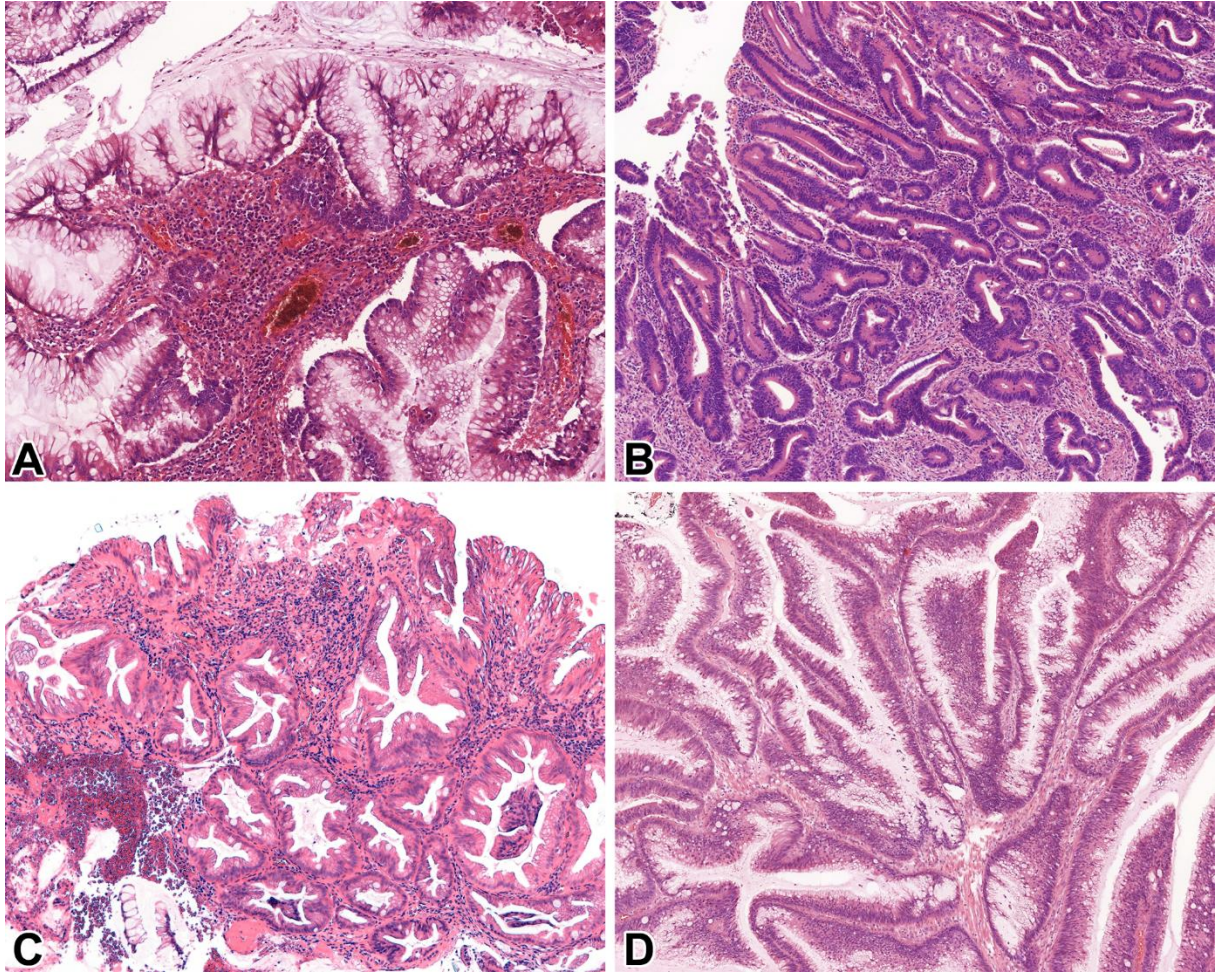


Figure 3 Microscopic features of IBD-associated NCDs of the examined population. (A): Hypermucinous dysplasia (10x, HE), (B): GCD (10x, HE), (C): Serrated dysplasia, NOS (10x, HE), (D): TSA-like dysplasia (10x, HE).

The cooccurrence of multiple NCD subtypes within the same case was common ($n = 9/17$; 53% of all cases with NCD) in resection specimens. The following combinations were observed: hypermucinous and serrated lesion, NOS ($n = 4$), hypermucinous and GCD ($n = 2$), hypermucinous, GCD, and TSA-like ($n = 1$), GCD and serrated lesion, NOS ($n = 1$), GCD and TSA-like ($n = 1$). Half of the 8 cases with only biopsy samples available showed exclusively conventional, while the other half demonstrated exclusively NCD. None of the included cases in our cohort had a concurrent or prior histologically proven endoscopically non-visible dysplasia in other bowel segments. Regarding the IBD-associated adenocarcinomas, they were histologically characterised as conventional ($n = 8$) and medullary ($n = 3$) in the exclusively conventional, and conventional ($n = 4$) and mucinous ($n = 4$) in the exclusively NCD cases. All mixed cases were associated with conventional adenocarcinomas ($n = 9$) (Table 1). A significant association ($p = 0.014$) was found between NCD and adenocarcinoma subtypes, and the proportion of NCD was significantly different ($p = 0.041$) within mucinous and medullary

subtypes. Most examined adenocarcinomas were low-grade (grade 2) in all groups (64% in the exclusively conventional dysplasia, 63% in the exclusively NCD, and 56% in the mixed group). Regarding stage, most cases were diagnosed as pT3 in the exclusively conventional dysplasia ($n = 7$) and the mixed group ($n = 7$), while the adenocarcinomas with exclusively NCD proved to be mostly T4 ($n = 4$). Right colon localisation was observed in 5 adenocarcinomas associated with conventional and 5 adenocarcinomas associated with NCD, while the left colon was affected in 6 cases with adjacent conventional and 3 cases with adjacent NCD. In the cases associated with mixed dysplasia, left colon localisation was observed in 5, and right colon localisation was seen in 4 patients. No significant association was found between NCD and the grade ($p = 0.093$), stage ($p = 0.131$), and localisation ($p = 0.253$) of associated adenocarcinomas.

4.2. Evaluation of dysplasias associated with IBD – a single-center, retrospective, 5-year experience

4.2.A. General clinicopathologic characteristics

In our examined 5-year period, a total of 921 IBD patients were included, and 57 possessed dysplasia or carcinoma samples. The mean age of the patients was 63.7 years (median: 65; range: 33–94). A male predominance was observed ($n = 34$; 59.6%), and most patients were treated for UC ($n = 41$; 71.9%). In half of the cases, IBD affected the left colon ($n = 29$; 50.9%), while pancolitis was reported in 17 cases (29.8%). The average duration of IBD prior to the diagnosis of neoplasia was 15 years (median: 14, range: 1–37).

4.2.B. Clinicopathologic characteristics of IBD associated conventional dysplasias

Altogether 47 patients were identified with conventional dysplasias. The average age of patients was 65.2 years (median: 66, range: 33–94), and male predominance was observed with a male-to-female ratio proved to be 31:16. Patients were mostly diagnosed with UC ($n = 33$; 70.2%), with left colon localization ($n = 22$; 46.8%), followed by pancolitis ($n = 15$; 31.9%). The average IBD duration until dysplasia diagnosis was 14.8 years (median: 14; range: 1–37). The dysplastic lesions were mainly identified in the left colon ($n = 31$; 65.9%). The average microscopic size of dysplasia was 0.66 cm (median: 0.5; range: 0.2–2.5), with mostly polypoid endoscopic morphology ($n = 34$; 72.3%). The dominant histological pattern proved to be tubular adenoma in the majority of cases ($n = 38$; 80.8%), and tubulovillous adenoma was solely found in 9 cases

(19.1%). Villous adenoma was not identified. Figure 4 represents conventional dysplasias found in our cohort.

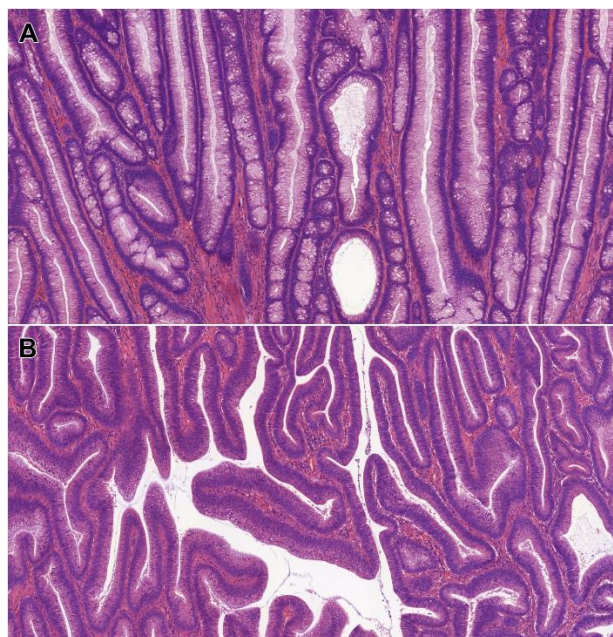


Figure 4 Microscopic features of IBD-associated, conventional dysplasias. (A): IBD-associated tubular adenoma with low-grade dysplasia (HE, 5x). (B): IBD-associated tubulovillous adenoma with low-grade dysplasia (HE, 5x).

Forty cases (85.1%) were defined as low-grade. The clinicopathological features of the identified conventional dysplasias are summarized in Table 2. A significant association was found between conventional dysplasias and dysplasia localization ($p = 0.004$), size ($p = 0.012$), endoscopic appearance ($p = 0.006$), grade ($p = 0.011$), macroscopic appearance of colorectal carcinoma ($p = 0.009$), and pT stage ($p = 0.01$). There was no association found with the patient's age ($p = 0.081$), gender ($p = 0.072$), subtype ($p = 0.708$), duration ($p = 0.817$) and extent of IBD ($p = 0.465$), development ($p = 0.058$), localization ($p = 0.064$), size ($p = 0.066$), grade ($p = 0.066$), multiplicity ($p = 0.619$), histological subtype ($p = 0.065$), pN ($p = 1.00$) and pM stage ($p = 0.208$) of colorectal carcinoma, the presence of lymphovascular invasion ($p = 1.00$), and microsatellite status ($p = 1.00$).

	Tubular adenoma (n=38)	Tubulovillous adenoma (n=9)
Age at diagnosis (years)	Mean: 64 Median: 63 (33–94)	Mean: 70 Median: 67 (62–81)
Male-to-female ratio	26:12	5:4
Type of IBD (n)	UC: 28 CD: 10	UC: 5 CD: 4
Localization of IBD (n)	Left colon: 19 Right colon: 8 Pancolitis: 11	Left colon: 3 Right colon: 2 Pancolitis: 4
Duration of IBD (years)	Mean: 14.8 Median: 12 (1–37)	Mean: 17.9 Median: 19 (9–24)
Localization of dysplasia (n)	Left colon: 26 Right colon: 12	Left colon: 5 Right colon: 4
Grade of dysplasia (n)	Low-grade: 36 High-grade: 2	Low-grade: 9 High-grade: 0
Size of dysplasia (cm)	Mean: 0.7 Median: 0.5 (0.2–2.5)	Mean: 0.47 Median: 0.4 (0.3–1.1)
Endoscopic appearance of dysplasia (n)	Polypoid: 26 Flat: 12	Polypoid: 8 Flat: 1
Association with NCD (n)	15	0
Association with adenocarcinoma (n)	11	1

Table 2 Clinicopathological characteristics of the identified conventional dysplasias.

4.2.C. Evaluation of IBD-associated adenocarcinomas in patients with conventional dysplasia

Of the 47 patients with conventional dysplasia, 12 patients (25.5%) were diagnosed with colorectal adenocarcinoma during follow-up, that were mainly localized to the left colon (n = 8; 66.7%), with average size of 4 cm (median: 3.75; range: 1–8.4), and infiltrative morphology (n = 7; 58.3%). The majority were identified as low-grade (n = 10; 83.3%). In half of the cases (n = 6), multiple colorectal carcinomas developed. Histologically, 7 cases (58.3%) were characterized as conventional adenocarcinoma, followed by mucinous (n = 3; 25%), signet ring cell (n = 1; 8.3%), and GCD (n = 1; 8.3%) patterns. Altogether 8 cases (66.7%) were found in T3 or T4 stage. Lymphovascular invasion and distant metastases were both identified in 3-3 cases (25%), respectively. Microsatellite instability (MSI) was identified in a single case (n = 1; 8.3%).

4.2.D. Clinicopathologic characteristics of IBD associated NCD

Among the 57 IBD patients with neoplastic samples, NCD was observed in 20 cases (35.1%). The mean age of these patients was 64.8 years (median: 66, range: 46–83), with a male-to-female ratio of 12:8. Most patients with NCD were diagnosed with UC (n = 14; 70%), and IBD was predominantly localized to the left colon (n = 11; 55%). The average time from IBD diagnosis to the detection of dysplasia was also 15 years (median: 15, range: 4–28). Most dysplastic lesions were localized to the left colon (n = 17; 85%), with average size of 0.59 cm (median: 0.45; range: 0.2–2.5), and mostly flat endoscopic morphology (n = 12; 60%). The predominance of them were histologically evaluated as low-grade (n = 15; 75%). Serrated dysplasia, NOS proved to be the most frequently observed subtype of NCD (n = 6; 30%), followed by hypermucinous (n = 4; 20%) GCD (n = 4; 20%) SSL-like (n = 2; 10%), and TSA-like dysplasia (n = 1; 5%). The clinicopathological features of the identified NCDs are summarized in Table 3. Serrated epithelial changes (SEC) were identified in 3 cases (15%). Since SEC is not unequivocally classified as dysplasia in current guidelines, these lesions are not included in the table. Figure 5 represents the identified histological subtypes.

	Serrated dysplasia, NOS (n=6)	Hypermucinous dysplasia (n=4)	GCD (n=4)	SSL-like dysplasia (n=2)	TSA-like dysplasia (n=1)
Age at diagnosis (years)	Mean: 64.8 Median: 66 (56–74)	Mean: 65 Median: 66 (48–83)	Mean: 56.8 Median: 55 (50–72)	Mean: 51.5	70
Male-to-female ratio	3:3	3:1	1:3	2:0	1:0
Type of IBD (n)	UC: 5 CD: 1	UC: 4 CD: 0	UC: 3 CD: 1	UC: 1 CD: 1	UC: 1 CD: 0
Localization of IBD (n)	Left colon: 5 Right colon: 1 Pancolitis: 0	Left colon: 0 Right colon: 0 Pancolitis: 4	Left colon: 2 Right colon: 1 Pancolitis: 1	Left colon: 1 Right colon: 0 Pancolitis: 1	Left colon: 0 Right colon: 0 Pancolitis: 1
Duration of IBD (years)	Mean: 15.6 Median: 15 (4–21)	Mean: 15.9 Median: 15 (9–28)	Mean: 16.6 Median: 16 (8–26)	Mean: 20	Mean: 9
Localization of dysplasia (n)	Left colon: 5 Right colon: 1	Left colon: 4 Right colon: 0	Left colon: 2 Right colon: 2	Left colon: 2 Right colon: 0	Left colon: 1 Right colon: 0
Grade of dysplasia (n)	Low-grade: 5 High-grade: 1	Low-grade: 4 High-grade: 0	Low-grade: 4 High-grade: 0	Low-grade: 2 High-grade: 0	Low-grade: 1 High-grade: 0
Size of dysplasia (cm)	Mean: 0.59 Median: 0.45 (0.3–2.4)	Mean: 0.55 Median: 0.4 (0.5–1.6)	Mean: 0.73 Median: 0.5 (0.3–1.4)	Mean: 0.65	Mean: 0.40
Endoscopic appearance of dysplasia (n)	Polypoid: 6 Flat: 1	Polypoid: 2 Flat: 2	Polypoid: 1 Flat: 3	Polypoid: 2 Flat: 0	Polypoid: 0 Flat: 1
Association with conventional dysplasia (n)	4	3	3	1	1
Association with other NCDs (n)	0	2	3	1	1
Association with adenocarcinoma (n)	4	2	4	1	0

Table 3 Clinicopathological characteristics of the identified NCDs.

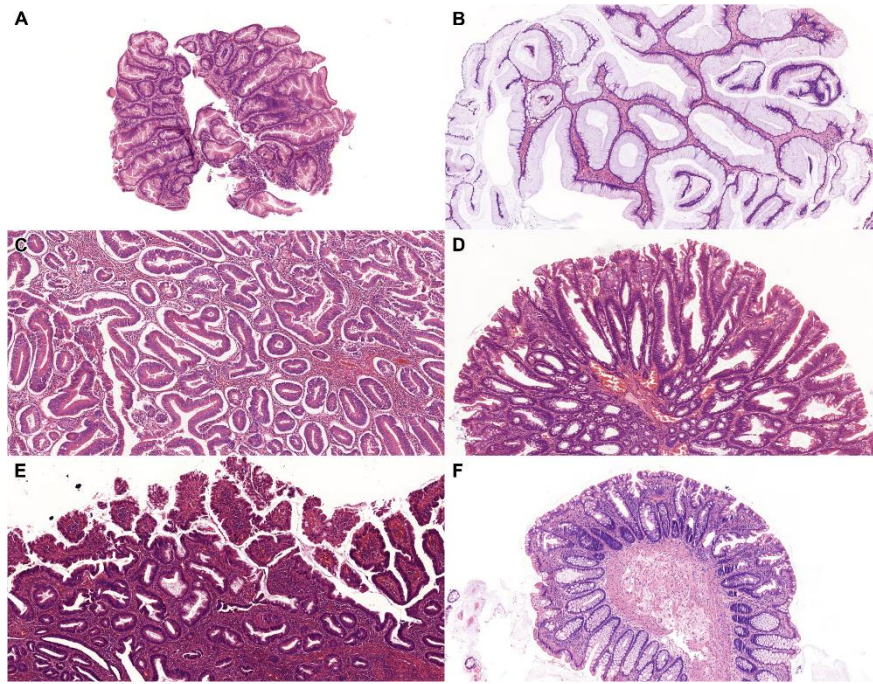


Figure 5 Microscopic features of IBD-associated, NCDs. (A): Serrated lesion, NOS (HE, 5x). (B): Hypermucinous dysplasia (HE, 5x). (C): GCD (HE, 5x). (D): SSL-like dysplasia (HE, 5x). (E): TSA-like dysplasia (HE, 5x). (F): SEC (HE, 5x).

A significant association was observed between the development of NCD and co-occurrence ($p < 0.001$), localization ($p = 0.001$), size ($p = 0.002$), macroscopic appearance ($p = 0.01$), grade ($p = 0.005$), histological subtype ($p = 0.003$), pT stage ($p = 0.003$), pM stage ($p = 0.047$) of colorectal carcinoma and microsatellite status ($p < 0.001$). However, no significant associations were found between NCDs and patient age ($p = 0.396$), gender ($p = 0.968$), type ($p = 0.319$), duration ($p = 0.481$), and extent of IBD ($p = 0.415$), macroscopic appearance ($p = 0.145$), and grade of NCD ($p = 0.865$), pN stage of invasive carcinoma ($p = 0.039$), or the presence of lymphovascular invasion ($p = 0.119$).

4.2.E. Evaluation of IBD-associated adenocarcinomas in patients with NCD

Out of the 20 patients with NCD, 12 (60%) developed colorectal adenocarcinoma during follow-up. Altogether 75% of tumors were located in the left colon ($n = 9$). The detected adenocarcinomas were predominantly classified as low-grade ($n = 11$; 91.7%). Histologically, the majority of these cancers were conventional adenocarcinomas ($n = 8$; 66.7%), followed by mucinous ($n = 2$; 16.7%), GCD ($n = 1$; 8.3%), and signet ring cell carcinomas ($n = 1$; 8.3%). The average tumor size was 3.64 cm (median: 3.5; range: 0.2–7.5). Macroscopic examinations most frequently revealed a polypoid morphology ($n = 7$; 58.3%), followed by sessile ($n = 3$; 25%) and flat lesions ($n = 2$; 16.7%). Tumors were identified as T1 ($n = 2$; 16.7%), T2 ($n = 3$;

35%), T3 (n = 4; 33.3%), and T4 (n = 3; 25%), respectively. Nodal involvement was observed only in N1 and N2 stages (n = 1; 8.3% and n = 2; 16.7%). Distant metastases were detected in 4 cases (33.3%). Immunohistochemical analysis of microsatellite status was performed in 14 cases. MSI was identified in 1 case (8.3%), while 7 cases (58.3%) reflected mismatch repair (MMR) proficiency. In the remaining 4 cases, no immunohistochemical or molecular genetic testing was performed.

4.2.F. Clinicopathologic characteristics of IBD associated, combined conventional dysplasia and NCD

Conventional dysplasia and NCD combined were identified in 15 cases (25.3%). The mean age of patients was 61.2 years (median: 58; range: 46–83). Male predominance was observed (n = 9; 75%), and most patients were treated with UC (n = 11; 73.3%). Patients were diagnosed with dysplasia 14.5 years after IBD diagnosis (median: 16; range: 5–28 years). UC affected the left colon in 8 cases (53.3%), and dysplasia was localized to the left colon in the majority of cases (n = 12; 80%). The average size of dysplasia proved to be 0.86 cm (median: 0.6; range: 0.2–2.5). In 8 cases (53.3%), the dysplasia appeared as polypoid during the endoscopic examination, while it remained flat in the rest of the cases (n=7; 46.7%). A significant association was found between the copresence of conventional dysplasias and NCDs and dysplasia size ($p = 0.045$), development ($p = 0.025$), localization ($p = 0.032$), macroscopic appearance ($p = 0.047$), multifocality ($p = 0.017$), histological subtype of colorectal carcinoma ($p = 0.033$), pT ($p = 0.014$), pN stage ($p = 0.012$), and microsatellite status ($p = 0.002$). There was no significant association observed with patient's age ($p = 0.37$), gender ($p = 0.684$), subtype ($p = 0.735$), duration ($p = 0.158$), and extent of IBD ($p = 0.468$), localization ($p = 0.19$), grade ($p = 0.224$), and macroscopic appearance of dysplasia ($p = 0.286$), size ($p = 0.056$) and grade ($p = 0.052$) of colorectal carcinoma, pM stage ($p = 0.089$), and the presence of lymphovascular invasion ($p = 0.057$).

4.2.G. Evaluation of IBD-associated adenocarcinomas in patients with combined conventional dysplasias and NCD

Nine (15.8%) patients who acquired both conventional and NCDs were diagnosed with colorectal carcinoma during follow up. The average age of patients at neoplasia diagnosis proved to be 61.6 years (median: 56; range: 46–83). The male-to-female ratio was 6:3. In

accordance with the above-detailed results, most patients (n=5; 55.6%) were diagnosed with UC, and IBD extent was observed either in the left colon (n=5; 55.6%), or as pancolitis (n=3; 33.3%). On average, patients were treated with IBD for 15.3 years before any kind of dysplasia diagnosis (median:15.5; range: 5–26). The carcinoma was mostly localized to the left colon (n=6; 66.6%), with average size of 3.7 cm (median: 3.8; range: 0.2–7.5). During the grossing examination, the majority of carcinomas were observed infiltrative (n=6; 66.6%) and were identified histologically as low-grade (n=8; 88.9%). Multiplicity was observed in 5 cases (55.6%) during follow-up. The most common histological subtype proved to be conventional adenocarcinoma (n=5; 55.6%), followed by mucinous (n=2; 22.2%), signet ring cell (n=1; 11.1%), and GCD (n=1; 11.1%) patterns. These carcinomas were mostly identified in an advanced, pT3 or pT4 stage (n=7; 77.8%), with lymph node and distant metastasis observed in 3-3 cases, respectively (33.3%; 33.3%). MSI was identified in a single case (11.1%).

4.2.H. Survival analysis

Kaplan-Meier analysis was performed to determine survival estimates (Figures 6–8). In patients with conventional dysplasia, there was no significant association found either in PFS ($p = 0.688$) or in OS ($p = 0.667$). Similar results were observed in patients with NCD in PFS ($p = 0.103$) and OS ($p = 0.167$), and in combined cases ($p = 0.596$ in PFS, and $p = 0.083$ in OS), respectively. The reason for that may lie in the fact that the cases comprising this study were procured in a period when NCDs were not yet discovered, therefore, random biopsy sampling was not yet widely applied. The other possible explanation may be the relatively short period of follow-up, therefore, the authors not only plan to expand the database, but plan to reperform the survival analysis in 5 and 10 years, as well.

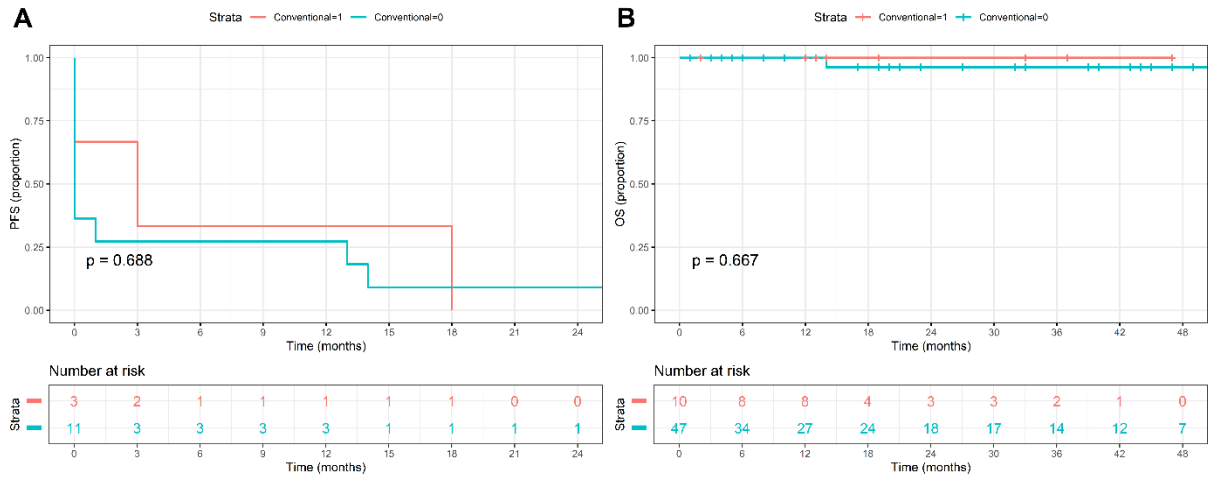


Figure 6 Kaplan-Meier estimates of PFS (A) and OS (B) in patients with conventional dysplasia.

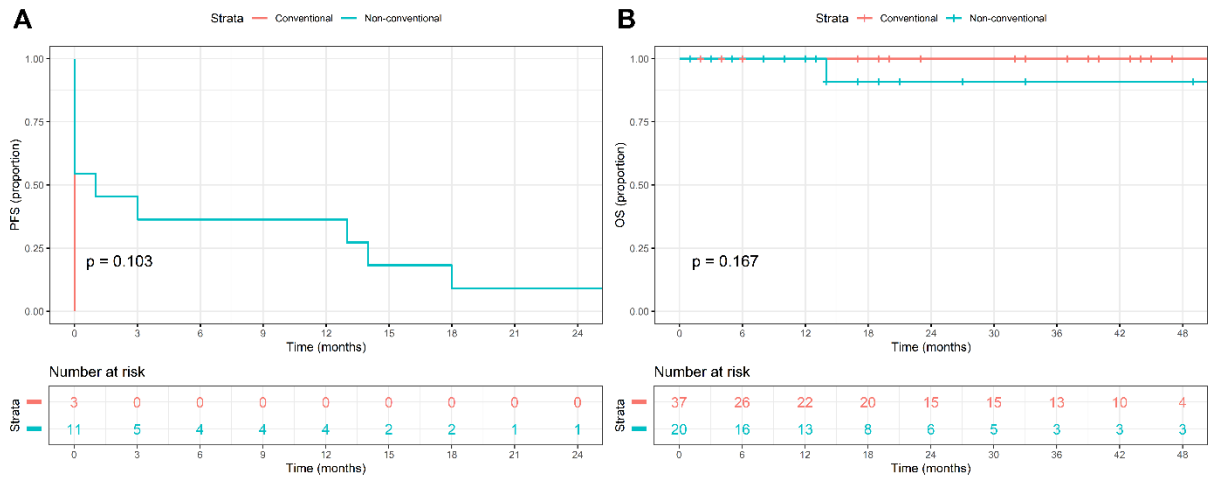


Figure 7 Kaplan-Meier estimates of PFS (A) and OS (B) in patients with NCD.

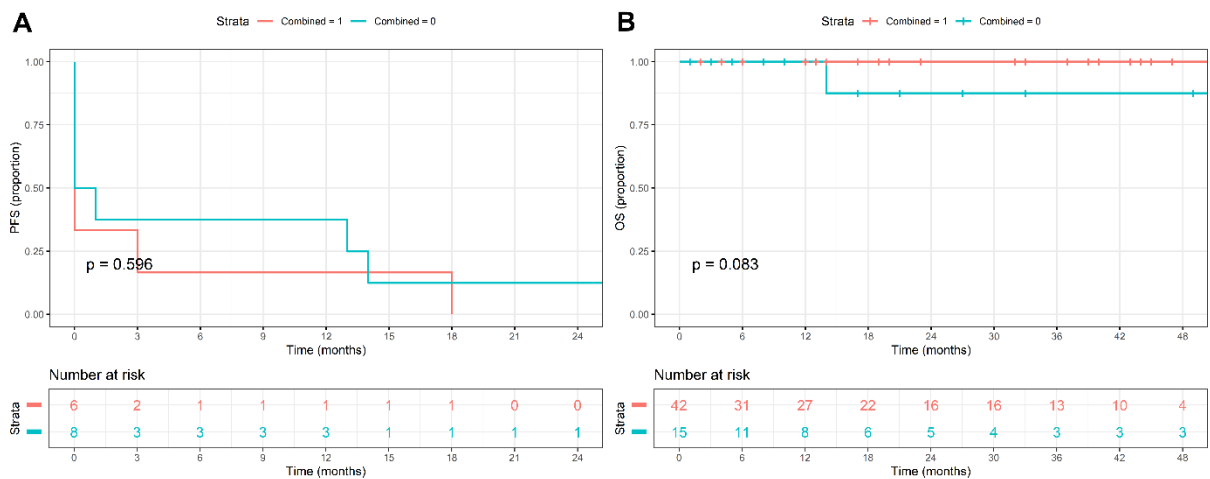


Figure 8 Kaplan-Meier estimates of PFS (A) and OS (B) in patients with combined conventional and NCD.

4.3. WES analysis of IBD-associated serrated dysplasia

4.3.A. Clinicopathologic features of serrated dysplasia

Table 4 summarizes the clinicopathologic features of the 11 IBD patients who developed 13 serrated dysplastic lesions. The mean age at the time of the serrated dysplasia diagnosis was 56 years (range: 35–71). Serrated dysplasia occurred predominantly in men (n = 8; 73%). Ten (91%) patients were diagnosed with UC, and 1 (9%) patient had CD. Pancolitis was observed in 7 (64%) patients, whereas the remaining 4 (36%) patients had left-sided colitis. The mean duration of IBD at the time of serrated dysplasia diagnosis was 26 years (range: 5–59). No patient had a concurrent history of PSC.

	Serrated dysplasia (n = 13, from 11 patients)
Mean age (years, range)	56 (35–71)
Male gender (%)	8 (73%)
IBD subtype (%)	UC: 10 (91%); CD: 1 (9%)
Extent of IBD (%)	Pancolitis: 7 (64%); Left-sided: 4 (36%)
Mean duration of IBD (years, range)	26 (5–59)
PSC (%)	0 (0%)
Subtype of serrated dysplasia (%)	SSL-like dysplasia: 5 (38%) TSA-like dysplasia: 1 (8%) Serrated dysplasia, NOS: 6 (46%) Mixed SSL-like/TSA-like dysplasia: 1 (8%)

Table 4 Clinicopathologic features of the IBD patients with serrated dysplasia.

Of the 13 serrated dysplastic lesions, 5 (38%) exhibited characteristics of SSL-like dysplasia, 1 (8%) showed features of TSA-like dysplasia, 6 (46%) were classified as serrated dysplasia, NOS, and 1 (8%) displayed mixed features of SSL-like and TSA-like dysplasias (Tables 4 and 5; Figure 1). Most lesions (n = 9; 69%) were found in the left colon, including SSL-like dysplasia (3/5; 60%) and serrated dysplasia, NOS (5/6, 83%). Eleven (85%) lesions had a polypoid endoscopic appearance, while the remaining 2 lesions, including 1 serrated dysplasia, NOS and 1 mixed SSL-like/TSA-like dysplasia, had a flat endoscopic appearance. The mean size of the lesions was less than 1 cm, except for the serrated dysplasia, NOS (mean: 1 cm, range: 0.3–2.5). The SSL-like dysplasia predominantly showed low-grade dysplasia (4/5; 80%), whereas half of the serrated dysplasia, NOS cases (3/6; 50%) displayed high-grade dysplasia. Among the 5 patients with either SSL-like dysplasia or serrated dysplasia, NOS, 1 (20%) also presented with conventional dysplasia. However, NCD was more frequently associated with the serrated dysplasia, NOS (3/5; 60%) than with the SSL-like dysplasia (1/5; 20%). During the

follow-up, 5 (45%) of the 11 patients developed CRC, including 3 patients with the serrated dysplasia, NOS, 1 with the SSL-like dysplasia, and 1 with the TSA-like dysplasia. The median PFS was 22 months (range: 1–64) in the SSL-like dysplasia group and 15.8 months (range: 1–51) in the serrated dysplasia, NOS group, and proved to be 1 month in the patient diagnosed with TSA-like dysplasia and 36 months in the mixed SSL-like/TSA-like dysplasia patient. In the case of the median OS, 34.6 months (range: 1–64) and 41 months (19–73) were established in the SSL-like dysplasia and serrated dysplasia, NOS groups, respectively, while 17 and 51 months were recorded for the TSA-like dysplasia and the mixed SSL-like/TSA-like dysplasia patients.

	SSL-like dysplasia (n = 5, from 5 patients)	Serrated dysplasia, NOS (n = 6, from 5 patients)	TSA-like dysplasia (n = 1, from 1 patient)	Mixed SSL-like/TSA-like dysplasia (n = 1, from 1 patient)
Mean age (years, range)	56 (35-71)	52 (36-63)	53	71
Male gender (%)	3 (60%)	4 (80%)	1 (100%)	1 (100%)
IBD subtype (%)	UC: 5 (100%) CD: 0 (0%)	UC: 4 (80%) CD: 1 (20%)	UC: 1 (100%) CD: 0 (0%)	UC: 1 (100%) CD: 0 (0%)
Extent of IBD (%)	Pancolitis: 4 (80%) Left-sided: 1 (20%)	Pancolitis: 3 (60%) Left-sided: 2 (40%)	Pancolitis: 0 (0%) Left-sided: 1 (100%)	Pancolitis: 1 (100%) Left-sided: 0 (0%)
Mean duration of IBD (years, range)	31 (5-59)	30 (7-47)	44	8
Location of dysplasia (%)	Left: 3 (60%) Right: 2 (40%)	Left: 5 (83%) Right: 1 (17%)	Left: 1 (100%) Right: 0 (0%)	Left: 0 (0%) Right: 1 (100%)
Endoscopic appearance of dysplasia (%)	Polypoid: 5 (100%) Flat: 0 (0%)	Polypoid: 5 (83%) Flat: 1 (17%)	Polypoid: 1 (100%) Flat: 0 (0%)	Polypoid: 0 (0%) Flat: 1 (100%)
Mean size of dysplasia (cm, range)	0.5 (0.2-0.9)	1.0 (0.3-2.5)	0.6	0.5
Histologic grade of dysplasia (%)	LGD: 4 (80%) HGD: 1 (20%)	LGD: 3 (50%) HGD: 3 (50%)	LGD: 0 (0%) HGD: 1 (100%)	LGD: 1 (100%) HGD: 0 (0%)
Association with conventional dysplasia (%)	1 patient with TA-like dysplasia (20%)	1 patient with TVA-like dysplasia (20%)	0 patient (0%)	1 patient with TA-like dysplasia (100%)
Association with NCD (%)	1 patient with mixed SSL-like/TSA-like dysplasia (20%)	2 patients with hypermucinous dysplasia (40%) 1 patient with GCD (20%)	0 patient (0%)	1 patient with SSL-like dysplasia (100%)
Association with CRC (%)	1 patient (20%)	3 patients (60%)	1 patient (100%)	0 patient (0%)

Table 5 Clinicopathologic features of the serrated dysplastic subtypes.

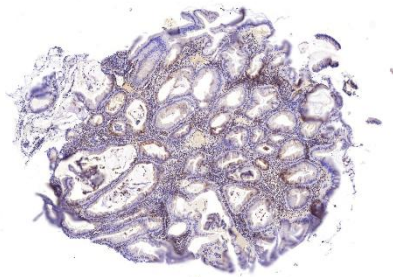
4.3.B. Molecular features of serrated dysplasia

WES was performed on 8 serrated dysplastic lesions from 7 patients (Table 6). For the remaining 5 lesions, either paraffin blocks were unavailable or the samples were unsuitable for WES. The SSL-like dysplasia in patient #5 harbored a likely pathogenic variant in *MLH1*, along with a high number of pathogenic and likely pathogenic variants, most of which were small frameshift insertions or deletions, which is suggestive of a MSI. Among these, a *KRAS* p.G12C mutation and 2 mutations in *PTEN* were identified. Consistent with the *MLH1* mutation in patient #5, the immunohistochemistry for MLH1 and PMS2 showed a loss of staining, confirming MSI (Figure 9A). Also, the SSL-like dysplasia in patient #3 showed an inactivating variant in *POLE*; however, this lesion did not exhibit a high number of mutations, suggesting that this variant is likely a passenger mutation rather than a driver mutation. Furthermore, the SSL-like dysplasia in patient #1 demonstrated a *BRAF* p.V600E mutation, whereas a class 3 *BRAF* mutation (p.G469A) was identified in the serrated dysplasia, NOS in patient #8. Both the SSL-like dysplasia (patients #1, #3, and #5) and serrated dysplasia, NOS (patients #4 and #8) showed likely pathogenic variants in *KMT2C* or *EXT1*. However, mutations in *TP53* or *POLG* were found only in the serrated dysplasia, NOS (patients #8 and #11, respectively). In line with the *TP53* mutation in patient #8, immunohistochemistry for p53 showed overexpression (Figure 2B). Patient #6, who had both SSL-like dysplasia and mixed SSL-like/TSA-like dysplasia, exhibited a pathogenic mutation in *MUTYH* (p.R217H), along with mutations in *MADD*.

Patient #	Subtype	Pathogenic mutations	Likely pathogenic mutations
1	SSL-like dysplasia	<i>BRAF</i> , <i>ATR</i>	<i>KMT2C</i>
3	SSL-like dysplasia	<i>EXT1</i>	<i>POLE</i> , <i>CDKN1B</i>
4	Serrated dysplasia, NOS	-	<i>KMT2C</i> , <i>MAX</i> , <i>CDC6</i>
5	SSL-like dysplasia	<i>KRAS</i> , <i>PTEN</i> , <i>TSC1</i>	<i>MLH1</i> , <i>DICER1</i> , <i>HIF1A</i> , <i>ASXL1</i> , <i>ZNF292</i> , <i>EXT1</i> , <i>ACVR2A</i> , <i>KMT2C</i> , <i>MGA</i> , <i>SETD1B</i> , <i>TGFBR2</i>
6 (le-sion #1)	SSL-like dysplasia	<i>MUTYH</i> , <i>MADD</i>	<i>SERPINB4</i>
6 (le-sion #2)	Mixed SSL-like/TSA-like dysplasia	<i>MUTYH</i> , <i>MADD</i>	-
8	Serrated dysplasia, NOS	-	<i>TP53</i> , <i>BRAF</i> , <i>MPL</i> , <i>EXT1</i>
11	Serrated dysplasia, NOS	<i>POLG</i>	-

Table 6 Molecular features of serrated dysplasia. Abbreviations: *ACVR2A* - Activin A receptor type 2A; *ASXL1* - Additional sex combs like 1; *ATR* - Ataxia telangiectasia and rad3-related; *CDC6* - Cell division cycle 6; *CDKN1b* - Cyclin-dependent kinase inhibitor 1B; *EXT1* - Exostosin glycosyltransferase 1; *HIF1A* - Hypoxia-inducible factor 1-alpha; *KMT2C* - Lysine N-methyltransferase 2C; *MADD* - MAP kinase-activating death domain; *MAX* - MYC-associated factor X; *MGA* - MAX dimerization protein MGA; *MPL* - Myeloproliferative leukaemia virus gene; *MUTYH* - MutY DNA glycosylase; *POLE* - Polymerase epsilon; *POLG* - DNA polymerase subunit gamma; *SERPINB4* - Serine proteinase inhibitor, clade B; *SETD1B* - SET domain containing 1B; *TGFBR2* - Transforming growth factor beta receptor 2; *TSC1* - Tuberous sclerosis 1; *ZNF292* - Zinc finger protein 292.

A



B

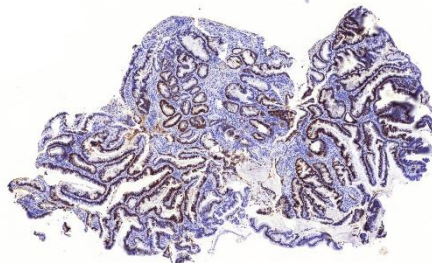


Figure 9 Immunohistochemical analysis of SSL-like dysplasia and serrated dysplasia, NOS. (A) *MLH1* immunohistochemistry shows a loss of staining in SSL-like dysplasia. (B) *p53* immunohistochemistry demonstrates overexpression in serrated dysplasia, NOS.

5. DISCUSSION

5.1. Examination of NCDs adjacent to colorectal adenocarcinoma in patients with IBD

The literature review was carried out using PubMed search and the keywords “inflammatory bowel disease,” “non conventional dysplasia,” and “non-conventional dysplasia”. The classification of IBD-associated dysplasias has changed over the past years. The Riddell classification (negative, indefinite, low-grade, and high-grade) from 1983 has been the gold standard for years; however, new subtypes, including villous and hypermucinous have been introduced in 1999 [12, 30]. The serrated subtype was first identified by Patil et al in 2017 [31]. A more recent and comprehensive classification has been published by Choi et al with 7 NCD subtypes, including hypermucinous, DPD, GCD, CCD, SSL-like, TSA like, and serrated dysplasia, NOS [13]. So far, there are 15 original studies in the literature examining these subtypes, of which 8 are retrospective and consecutive, with additional sporadic case presentations [11, 13-16, 18, 20, 23, 24, 32-38]. Most of the available literature focuses on colorectal pathology; however, counterparts associated with CD affecting the small intestine were also reported [39, 40]. NCD was detailed in 8 review articles [5, 6, 25-27, 41-43]. Based on our current knowledge, IBD-associated NCD may harbour aneuploidy, DNA abnormalities, and *p53* mutation (overexpressed or null phenotype) more frequently than conventional counterparts [14, 33]. Regarding their development, high inflammatory activity has been proven to be an independent risk factor, according to the results of Nguyen et al [32]. Musulen et al suggested gastric metaplasia as a candidate precursor lesion to some hypermucinous dysplasia, in accordance with the results of Kővári et al [36, 38]. Furthermore, NCD in general, is more commonly associated with UC and PSC [23, 26, 33]. In a North American population, DPD and CCD subtypes may be the most common [14]. Moreover, Bahceci et al demonstrated that CCD and GCD frequently present as flat or invisible lesions endoscopically, and most endoscopically undetected lesions were categorised as non conventional [15, 18]. A correlation between NCD subtypes and special histologic types of invasive adenocarcinoma was also proposed. GCD and hypermucinous subtypes have been identified as candidate precursor lesions of low-grade tubuloglandular and mucinous adenocarcinomas, respectively [16]. The presence of NCD has been associated with more frequent and earlier recurrence of intraepithelial neoplasia, larger lesion size, and high-grade adenocarcinomas [13, 34]. Overall, their molecular background, possibly flat or invisible morphology, and the high probability of relapse and high-grade features of associated adenocarcinomas all suggest an overall worse prognosis compared to conventional dysplasia. In most studies, the evaluation of NCD has been

mainly determined by 1 or 2 expert gastrointestinal pathologists [13, 14, 16, 23, 32, 33, 44]; therefore, the reproducibility of the new classification is uncertain. Although each included 6 evaluators, Choi et al's and Lang-Schwartz et al's studies did not report data on intraclass correlation. According to the results of Nasreddin et al, poor agreement was found between 6 evaluators using the same classification [35]. An even more detailed classification was published in 2023 by Harpaz et al, dividing IBD-associated dysplasias into intestinal (tubular/villous adenoma-like, GCD, CCD, TSA-like, SSL-like, serrated dysplasia, NOS), gastric (tubular/villous, serrated), and mixed categories. Reproducibility examination reflected good general agreement regarding definitive diagnosis [24]. Table 7 summarises the results of the literature review.

Author	Year of publication	Type of article	Type of study	Examined NCD subtypes	Number of cases	Number of evaluators	Types of specimens	Immunohistochemical analysis	Molecular analysis	New findings
Andersen et al [30]	1999	Original research	Retrospective, consecutive, unicenter	Hypermucinous, villous mucosa	13	Not mentioned	Colectomy	NA	<i>KRAS</i> mutation analysis	Highest <i>KRAS</i> mutation frequency was found in hypermucinous and villous mucosa.
Patil et al. [31]	2017	Original research	Retrospective	New classification: adenoma-like, terminally differentiated, serrated, hypermucinous	30	Not mentioned	Not mentioned	MUC2, MUC5AC, MUC6, p53, β -catenin, annexin A10, Maspin, BRAF, SOX9	NA	P53 plays a role in adenoma-like, terminally differentiated, and hypermucinous dysplasias. Combined alterations of p53 and β -catenin are observed in serrated precursors. MUC6 is a marker of hypermucinous subtype.
Kamarádová et al. [45]	2019	Original research	Retrospective, consecutive, unicenter	Putative precursor lesions (Serrated change/dysplasia, villous hypermucinous change)	309	Not mentioned	Colectomy	MMR, p53, MGMT	<i>KRAS</i> , <i>NRAS</i> , <i>BRAF</i> mutation analysis	IBD-associated adenocarcinomas are heterogenic. All putative precursor lesions are associated with longstanding IBD.
Kamarádová et al. [46]	2020	Original research	Retrospective, consecutive, unicenter	Putative precursor lesions (Serrated change/dysplasia, villous hypermucinous change)	309	Not mentioned	Colectomy	MLH1, p53, MGMT	<i>KRAS</i> , <i>NRAS</i> , <i>BRAF</i> mutation analysis	Almost half of IBD-associated NCDs may harbour <i>KRAS</i> mutations.

Choi et al. [13]	2020	Original research	Retrospective, multicenter	New classification: Hypermucinous, TSA-like, SSL-like, serrated dysplasia, NOS, DPD, GCD, CCD	58	6	Colectomy	NA	NA	Colorectal carcinomas associated with NCDs tend to be high-grade, and they mainly be found in the left colon.
Pereira et al. [27]	2020	Review	NA	NA	NA	NA	NA	NA	NA	NA
Lee et al. [14]	2021	Original research	Retrospective, consecutive, unicenter	Hypermucinous, TSA-like, SSL-like, serrated dysplasia, NOS, DPD, GCD, CCD	168	1 or 2	Biopsy, colectomy	NA	DNA flow cytometry	Almost half of NCDs may harbour aneuploidy, and they may present as flat lesions during endoscopic examination. DPD and CCD are the most commonly identified subtypes.
Choi [6]	2021	Review	NA	NA	NA	NA	NA	NA	NA	NA
Choi et al. [15]	2022	Original research	Retrospective, multicenter	Hypermucinous, CCD, GCD	126	1	Biopsy, colectomy	p53	NA	NCDs may predominantly be found in patients with UC, and may be associated with PSC in 1/4 of cases. CCD and GCD subtypes are often present as endoscopically flat or invisible lesions. P53 null or mutant phenotype may be found in 29-55% of cases.

Choi et al. [26]	2022	Review	NA	NA	NA	NA	NA	NA	NA	NA
Kamarádová [41]	2022	Review	NA	NA	NA	NA	NA	NA	NA	NA
Zhang et al. [23]	2022	Original research	Retrospective, consecutive, unicenter	Hypermucinous, TSA-like, SSL-like, serrated dysplasia, NOS, DPD, GCD, CCD	173	2	Biopsy, colectomy	NA	NA	Almost 1/3 of PSC-IBD patients may develop dysplasia, that is mostly characterized as non-conventional.
Nguyen et al. [32]	2022	Original research	Retrospective, consecutive, unicenter	Hypermucinous, TSA-like, SSL-like, serrated dysplasia, NOS, DPD, GCD, CCD	125	1	Biopsy	NA	NA	Higher inflammatory activity score increases the chance of the development of IBD-associated NCDs.
Bahceci et al. [44]	2022	Original research	Retrospective, consecutive, unicenter	Hypermucinous, TSA-like, SSL-like, serrated dysplasia, NOS, DPD, GCD, CCD	207	2	Biopsy, colectomy	NA	NA	Colonoscopically undetected dysplasias are mainly non-conventional.
Akarca et al. [16]	2023	Original research	Retrospective, consecutive, multicenter	Hypermucinous, TSA-like, SSL-like, serrated dysplasia, NOS, DPD, GCD, CCD	46	1	Colectomy	NA	NA	CCD and hypermucinous dysplasias are precursor lesions of low-grade tubuloglandular and mucinous adenocarcinomas.
Zhang et al. [33]	2023	Original research	Retrospective, consecutive, unicenter	Hypermucinous, TSA-like, SSL-like, serrated dysplasia, NOS, DPD, GCD, CCD	96	1	Biopsy	NA	DNA flow cytometry	PSC-IBD patients are more likely to developing dysplasias of the right colon, and DNA abnormality.
Choi [25]	2023	Review	NA	NA	NA	NA	NA	NA	NA	NA

Waters et al. [42]	2023	Review	NA	NA	NA	NA	NA	NA	NA	NA
Lang-Schwarz et al. [34]	2023	Original research	Retro- and prospective, consecutive, unicenter	Hypermucinous, DPD, GCD, CCD	5435	6	Not mentioned	NA	NA	NCDs are associated with more frequent and earlier relapse low-grade intraepithelial neoplasia relapse, and larger lesion size.
Almási et al. [11]	2023	Case report	NA	NA	NA	NA	NA	NA	NA	NA
Enea et al. [43]	2023	Review	NA	NA	NA	NA	NA	NA	NA	NA
Alipour and Stashek [5]	2023	Review	NA	NA	NA	NA	NA	NA	NA	NA
Harpaz et al. [24]	2023	Original research	Retrospective	New classification: intestinal dysplasia (tubular/villous adenoma-like, GCD, CCD, TSA-like, SSL-like, serrated dysplasia, NOS), gastric dysplasia (tubular/villous, serrated), and mixed	35	7	Not mentioned	NA	NA	The new classification system is reproducible, with 2/3 of cases with definitive diagnosis.

Guerini et al. [39]	2023	Original research	Retrospective, multicenter	TSA-like, GCD	49	2	Small bowel resection	CK7, CK20, MUC5AC, MUC6, CDX2, B-catenin, p53, MLH1, PMS2, MSH2, MSH6	<i>IDH1</i> mutation analysis and MGMT promoter methylation	<i>IDH1</i> -mutated, CD-associated small bowel adenocarcinomas represent a subtype with differing immunohistochemical and methylation profile. <i>IDH1</i> -mutated non-conventional, TSA-like dysplasia may be a precursor lesion of these tumours.
Nasreddin et al. [35]	2024	Original research	Retrospective, consecutive, unicenter	Hypermucinous, TSA-like, SSL-like, serrated dysplasia, NOS, DPD, GCD, CCD	89	6	Biopsy, colectomy	NA	NA	Poor agreement IBD-associated was found in IBD-associated NCD subtypes.
Musulen et al. [36]	2024	Original research	Retrospective, multicenter	Hypermucinous, TSA-like, SSL-like, serrated dysplasia, NOS, DPD, GCD, CCD, SEC	33	3	Colectomy	p53, MUC5AC, MLH1, CDX2	NA	On the basis of IBD, gastric metaplasia may develop, that serves as a precursor lesion of NCDs. The expression of MUC5AC decreases with the increase of the degree of dysplasia.

Our study	2024	Original research	Retrospective, randomized	Hypermucinous, TSA-like, SSL-like, serrated dysplasia, NOS, DPD, GCD, CCD	28	2	Biopsy, colectomy	NA	NA	IBD-associated NCDs may often appear combined, and the most common combination is hypermucinous and serrated dysplasia, NOS. NCDs are significantly associated with mucinous adenocarcinomas, while conventional subtypes are associated with medullary adenocarcinomas.
------------------	------	-------------------	---------------------------	---	----	---	-------------------	----	----	--

Table 7 Results of the literature review. Abbreviations: CDX2 - Caudal-type homeobox transcription factor 2; CK7 - Cytokeratin 7, CK20 - Cytokeratin 20; IDH1 - Isocitrate dehydrogenase 1; Maspin - Mammary serine protease inhibitor; MGMT - O(6)-Methylguanine-DNA-methyltransferase; MLH1 - MutL homolog 1; MSH2 - MutS homolog 2; MSH6 - MutS homolog 6; MUC2 - Mucin 2; MUC5AC - Mucin-5AC; MUC6 - Mucin 6; NA – Not applicable; NRAS - Neuroblastoma ras viral oncogene homolog; p53 - Tumour protein p53; PMS2 - PMS1 homolog 2; SOX9 - SRY-Box Transcription Factor 9

Hereby, we performed the first Hungarian pilot study, aiming to re-evaluate several IBD-associated adenocarcinoma cases to retrospectively survey the incidence of NCD and to validate that recent North American findings may apply to a Central-Eastern European population. We also provide an updated literature review. Our study successfully demonstrated the presence of NCD adjacent to 60% of 28 randomly selected IBD-associated colorectal adenocarcinoma cases diagnosed between 2010 and 2022 at the Department of Pathology, University of Szeged. Although our primary focus was identifying and subtyping adjacent NCDs, we also aimed to evaluate the most significant clinicopathological parameters. In our study, the most common subtype proved to be hypermucinous dysplasia, but interestingly, CCD and DPD subtypes were not found in the examined population, even though these subtypes are common in North American populations [13, 15, 26]. Nonetheless, DPD was reported to be typically low-grade and less frequently associated with advanced neoplasms, explaining its absence in our IBD-associated adenocarcinoma cohort [26]. Otherwise, discrepancies may be explained by the differing population or the non consecutive and pilot nature of our study design. Some examined clinicopathological parameters, including patients' age at the time of dysplasia diagnosis, the duration of IBD, and the association with UC reflect international literature data. Other prognostic factors of colorectal carcinomas showed varying distribution, likely due to the low number of cases; therefore, no significant association was found between these parameters. Although literature data support an association between the risk of NCD development and high histologic inflammatory activity, we failed to reproduce these findings, likely due to the lack of statistical power [32]. A significant association was found between adenocarcinoma subtypes and adjacent dysplasia subtypes. Mucinous adenocarcinomas were solely found in the NCD population, and medullary adenocarcinomas were only present in the conventional dysplasia group. Unexpectedly, all cases with mixed conventional and NCD components were associated with conventional adenocarcinomas ($n = 9$). This finding is discrepant from the results of earlier studies, which showed mixed dysplasia associated with both tubuloglandular and mucinous adenocarcinomas [16]. The recent studies of Kővári et al and Musulen et al may offer some explanation for these results, as some evidence suggests that a chronic inflammation-foveolar metaplasia-hypermucinous dysplasia-mucinous adenocarcinoma sequence may exist in the setting of IBD [36, 38]. The association of NCDs with UC was reproduced in our cohort. The limitation of our study, as expected from a pilot design, is the relatively small number of patients. We are currently working on a complete consecutive IBD-associated neoplasia cohort comprising all cases between 2010 and 2023. The selection of cases was random, and unexpectedly, all cases included dysplasia adjacent to the carcinoma. Based on our results,

either conventional, non-conventional or mixed, dysplasia is a common tumour-accompanying change in the setting of IBD. Although NCDs were reported to harbour molecular alterations characteristic of advanced neoplasia [14, 15], more detailed comparative molecular analysis of both the carcinomatous and dysplastic components are needed to establish that NCDs represent definite tumour precursor lesions. Of note, none of the included cases in our cohort had concurrent or prior histologically proven, endoscopically non-visible dysplasia. However, the retrospective nature of this study may explain the lack of such lesions. At the time of sampling, endoscopists were unaware of the implications of NCD and its association with flat and invisible endoscopic presentation. In most of our cases with prior or concurrent biopsies targeting other colonic segments, the samples were taken from endoscopically inflamed mucosa to determine disease activity, endoscopically visible lesions concerning for dysplasia, or represented limited step biopsies from endoscopically uninvolved mucosa. A further limitation is the lack of insight into the clinical management (i.e., the type of anti-inflammatory drug used for induction and maintenance of remission and the applied dosages), that may have had an impact on the ongoing inflammation-related mucosal injury and related carcinogenetic damage. International data and our results highlight the importance of recognising IBD-associated NCDs on the pathologists' side. At the same time, clinically, these patients may benefit from individualised follow-up and random biopsy sampling.

5.2. Evaluation of dysplasias associated with IBD – a single-center, retrospective, 5-year experience

Choi et al introduced a new classification of IBD-associated dysplasias, namely, NCDs [5]. The presence of NCDs is currently considered to predict a poorer prognosis, as they are more frequently associated with aneuploidy, high-grade dysplasias, and high-risk carcinomas. Some subtypes may appear flat during the endoscopic examination, making their detection challenging. Given the limited information about these lesions, their clinical and histological identification remains difficult. In our study, we reviewed the neoplastic specimens of IBD patients with histological samples from the University of Szeged (Hungary) between 2011 and 2015 to identify NCDs, to perform statistical analysis of clinicopathological factors potentially influencing prognosis, and to compare them with conventional dysplasias. During the study period, 57 patients were included in our database, with a mean age of 63.7 years (median: 65, range: 33–94), and male predominance ($n = 34$; 59.6%). The majority of patients were treated for UC ($n = 41$; 71.9%). Conventional dysplasias were observed in 47 patients. The average age proved to be 65.2 years (median: 66; range: 33–94), and male predominance was observed

in this group, as well (n = 31; 65.9%). Patients were mostly diagnosed with UC (n = 33; 70.2%), with left colon localization (n = 22; 46.8%). The average IBD duration until dysplasia diagnosis was 14.8 years (median: 14; range: 1–37). In accordance with IBD localization, dysplastic lesions were mainly identified in the left colon (n = 31; 65.9%). Altogether 12 patients (25.5%) were diagnosed with colorectal adenocarcinoma during follow-up, that were mainly localized to the left colon (n = 8; 66.7%). The majority were identified as low-grade (n = 10; 83.3%). In half of the cases (n = 6), multiplicity was observed, as well. Seven cases (58.3%) were characterized as conventional adenocarcinoma, followed by mucinous (n = 3; 25%), signet ring cell (n = 1; 8.3%), and GCD (n = 1; 8.3%) patterns. Most cases (n = 8; 66.7%) were found in an advanced, T3 or T4 stage. A significant association was found between the presence of conventional dysplasias and dysplasia localization, size, endoscopic appearance, grade, macroscopic appearance of colorectal carcinoma, and pT stage. In our cohort, NCDs were identified in 20 patients (35.1%), predominantly around the 6th decade of life, with a slight male predominance (n = 12; 60%), associated with UC (n = 14; 70%). Of note, UC, NCD subtypes, as well as colorectal adenocarcinomas, were predominantly localized to the left colon in this cohort. During revisional histological examination, serrated dysplasia, NOS was detected in 6 cases (30%), followed by hypermucinous (n = 4; 20%) GCD (n = 4; 20%), SSL-like (n = 2; 10%) and TSA-like dysplasia (n = 1; 5%). Out of the 20 cases, a total of 12 (60%) also developed colorectal adenocarcinoma, which was found to be predominantly low-grade (n = 11; 91.7%) and conventional adenocarcinoma subtype (n = 8; 66.7%). Rarer subtypes were also identified, however, as the association of non-conventional carcinoma subtypes with NCDs is not fully understood, further conclusions on this issue cannot be made. The majority of these adenocarcinomas were detected at advanced T3 and T4 stages (together n = 7; 58.3%), and 4 cases (33.3%) were diagnosed in M1 stage. A significant correlation was observed between NCDs and colorectal carcinoma development, localization, tumor size, macroscopic appearance, grade, histological subtype, pT and pM stage, and microsatellite status. Conventional dysplasias and NCDs were present combined in 15 cases (25.3%). In accordance with the above-mentioned data, the mean age of patients was 61.2 years (median: 58; range: 46–83), male predominance was observed (n = 9; 75%), and most patients were treated with UC (n = 11; 73.3%). Patients were diagnosed with dysplasia 14.5 years after IBD diagnosis (median: 16; range: 5–28 years). Altogether 9 patients (15.8%) were diagnosed with colorectal carcinoma, as well, that were identified as low-grade (n = 8; 88.9%), and in 5 cases (55.6%) as multiple. Several histological subtypes were identified, including conventional adenocarcinoma (n = 5; 55.6%), mucinous (n = 2; 22.2%), signet ring cell (n = 1; 11.1%), and GCD

adenocarcinoma (n = 1; 11.1%). A significant association was found between the co-presence of conventional dysplasias and NCDs and dysplasia size, development, localization, macroscopic appearance, multifocality, histological subtype of colorectal carcinoma, pT, pN stage, and microsatellite status. International findings and our work suggest that the detection of IBD-associated NCD may be a key issue in future gastrointestinal pathology, as it was found to be common in neoplastic specimens in our consecutive retrospective study (20/ 57; 35.1%). It is also important to emphasize that, based on the work of Choi et al, using North American data, several NCD subtypes are flat, making them difficult or impossible to detect endoscopically [13]. Among the patients involved in our study, the majority of NCDs were polypoid (n = 11; 55%); however, it must be noted that at the time of sampling NCD subtypes had not yet been described, so the samplers may not have been aware of the significance of potentially flat lesions. Furthermore, in our data, serrated dysplasia, NOS was found to be the most common, whereas the CCD and DPD subtypes observed in the US population were not identified at all. The different proportions of histological subtypes could account for the differences in endoscopic morphology. Based on our findings, the presence of NCD predisposes the development of colorectal adenocarcinoma and predicts a poorer prognosis, as it is associated with tumors of more advanced stages. Moreover, these tumors were predominantly found to be microsatellite stable, rendering them ineligible for treatment with Programmed Cell Death Ligand 1 inhibitors according to current guidelines [47]. Conventional dysplasias have already been widely investigated by many study groups during the last 4 decades, therefore, all the above-mentioned clinicopathological factors have been identified. On the other hand, NCDs have been identified in recent years, therefore, they have only been in the focus of attention for a short period, resulting in limited information. It must be emphasized that such consecutive, retrospective, cohort study has not been performed before in a Central European population. Furthermore, our study aimed to investigate cases with the co-occurrence of conventional dysplasias and NCDs, representing results as the first of their kind. With the emergence of novel morphological variants, the histopathological characteristics are not fully described, making their diagnosis particularly challenging. This complexity is compounded by the requirement of the confirmation of at least 2 gastrointestinal pathologists to diagnose IBD associated neoplasms, as stipulated by current international guidelines [48]. However, non-primary healthcare institutions may lack the necessary specialization, as well as access to advanced diagnostic tools such as immunohistochemistry and molecular genetic testing. Furthermore, the poor prognosis associated with IBD-related NCDs may be attributed to their higher rates of aneuploidy and their frequent association with high-risk carcinomas. Given these challenges,

some experts advocate for randomized biopsy sampling and more rigorous patient monitoring in cases of NCD [26]. In conclusion, IBD-associated NCDs require increased attention during histopathological evaluation. Larger cohort studies from Hungary and the Central European region are needed to gain a more comprehensive understanding of their clinical behavior. Based on current knowledge, patients may benefit from close follow-up involving endoscopic sampling, randomized biopsies, and, in cases where NCD is diagnosed, complete removal of the lesion is recommended [26].

5.3. WES analysis of IBD-associated serrated dysplasia

The clinicopathologic and molecular features of SSL-like dysplasia in IBD are not yet fully understood. In this regard, we note that SSL-like dysplasia was more frequently found in the left colon (60%) and in men (60%) (Table 2), in contrast to its sporadic counterpart, which is typically located in the right colon and more commonly affects women [49-54]. Also, the mean age of patients with SSL-like dysplasia (56 years) was lower than the reported age range for sporadic SSL with dysplasia (60–76 years). Furthermore, in addition to the typically observed *BRAF* mutation, the *MLH1* mutation was detected in a single case, which may rarely be detected in sporadic SSL with dysplasia [19, 51, 53]. WES identified mutations have not been previously reported in SSL with or without dysplasia, including *POLE*, *KMT2C*, and *EXT1*. Overall, these findings suggest that SSL-like dysplasia in IBD may represent a distinct entity compared with its sporadic counterpart. *POLE* plays a crucial role in the DNA proofreading mechanism, but its mutations are rare in CRC, occurring in approximately 3% of cases [55, 56]. These mutations are more commonly found in younger individuals, affect men more frequently than women, and are usually located in the right colon [55-57]. Notably, among Asian patients, 68% of *POLE* mutations are identified in the left colon, whereas 64% of non-Asian patients have them in the right colon ($p < 0.01$) [56]. *POLE* mutations are usually independent of *BRAF* and *KRAS* mutations, as well as MSI [55, 56]. The presence of *POLE* mutations in SSL-like dysplasia that lacks *BRAF*, *KRAS*, or *MLH1* mutations (patient #3; Table 3) suggests that a subset of SSL-like dysplastic lesions may serve as precursors for *POLE* mutant CRCs. Although *POLE*-mutant CRCs are generally considered a subtype with a favorable prognosis, they can exhibit high-grade histologic features, including poorly cohesive rhabdoid cells and areas resembling medullary carcinoma [55, 56, 58]. Similarly, mutations in genes involved in histone modification, such as *KMT2C*, are exceedingly rare in CRC, occurring in approximately 1% of cases, but are significantly more frequent in CRC affecting younger patients [59]. Meanwhile, *EXT1* is primarily recognized for its role in hereditary multiple exostoses (osteochondromas),

and the potential relevance of *EXT1* mutations in CRC remains unclear [60]. Of note, although rare, mutations in *KRAS* and *PTEN* have been observed in sporadic SSL with dysplasia. Bettington et al. identified *KRAS* mutations at codon 12 or 13 in 1 (1%) out of 137 SSLs with dysplasia, while Murakami et al. reported *PTEN* mutations in 1 (13%) out of 8 SSLs with dysplasia [51, 61]. Consistent with these findings, only 1 (25%) of the 4 SSL-like dysplastic lesions in our cohort had both mutations (patient #5) (Table 3). However, this lesion also exhibited a likely pathogenic variant in *MLH1*, along with a high number of pathogenic and likely pathogenic variants, most of which were small frameshift insertions or deletions, indicating MSI. Indeed, a previous study showed that mutations in various genes, including *PTEN*, could result from MSI in MSI-high CRCs [62]. Serrated dysplasia, NOS is a recently described subtype of serrated dysplasia that lacks the typical features of SSL-like dysplasia or TSA-like dysplasia. However, its clinicopathologic and molecular features are largely unknown. In this regard, we found that the serrated dysplasia, NOS predominantly occurred in the left colon (83%) and was more common in men (80%) (Table 2). Notably, the serrated dysplasia, NOS exhibited a higher frequency of high-grade dysplasia (50%) compared with the SSL-like dysplasia (20%). The serrated dysplasia, NOS was also more frequently associated with NCD (60%, including 2 cases of hypermucinous dysplasia and a single case of GCD) compared with the SSL-like dysplasia (20%, including one case of mixed SSL like/TSA-like dysplasia). NCD, including hypermucinous dysplasia, crypt dysplasia (which features mild cytologic atypia confined to the crypt bases), and GCD, is considered high risk because they are more frequently detected as flat/invisible dysplasia (42–100%) and associated with advanced neoplasia upon follow-up (40–93%) compared with conventional dysplasia or sporadic adenomas (18% and 10%, respectively) [14, 23, 26, 32, 33, 37, 44, 63]. Consistently, the serrated dysplasia, NOS demonstrated worse outcomes upon follow-up, with 3 of the 5 patients (60%) developing CRC. In addition to the mutations observed in the SSL-like dysplasia, such as *BRAF*, *KMT2C*, and *EXT1*, the serrated dysplasia, NOS exhibited mutations in *TP53* or *POLG*. Notably, a single case of serrated dysplasia, NOS (patient #8) harbored both *TP53* and *BRAF* mutations without *MLH1* mutations (Table 3), aligning with previous findings stating that *BRAF*-mutated microsatellite stable (MSS) CRCs frequently present with *TP53* mutations (41% vs. 17% in *BRAF*-mutated, MSI CRCs) and are considered the most aggressive molecular subtype [51, 64–66]. The significance of *POLG* mutations in another case of serrated dysplasia, NOS (patient #11), which are associated with a wide variety of mitochondrial diseases, remains uncertain, as they have not been previously linked to any serrated lesions. Linkowska et al. also found no evidence supporting a role for *POLG* mutations in driving the

accumulation of somatic mutations in mitochondrial DNA or in the development and progression of CRC [67]. However, more recently, using a mouse model of inflammation induced colon tumorigenesis, Maiuri et al. reported that inflammation-induced alterations in Polg expression may play a significant role in tumorigenesis by reducing mitochondria levels and altering metabolism, making the tumor more resistant to oxidative stress [68]. Taken together, these findings suggest that serrated dysplasia, NOS may have distinct molecular features compared with SSL-like dysplasia, and a subset of these lesions could represent precursor lesions for *BRAF*-mutated MSS CRCs, potentially explaining their higher malignant potential. A potential limitation of our study was that due to the very high number of the original cohort, solely patients with neoplasia diagnosis were reevaluated; therefore, samples may have been missed during the reevaluation process. Our findings support the fact that IBD-associated serrated lesions are often associated with CRC (45%), and therefore, may be later on defined in the serrated dysplasia category. Such lesions should be excised completely, and patients may benefit from a closer follow-up [18].

6. CONCLUSIONS

1. This first Hungarian pilot study investigated IBD-associated colorectal adenocarcinomas to assess the presence of NCD and compare findings with North American data. NCD was identified adjacent to 60% of cases, with hypermucinous dysplasia being the most common subtype. Mucinous adenocarcinomas were exclusively associated with NCD, and medullary types only with conventional dysplasia, suggesting distinct pathogenetic pathways. The results support a possible inflammation–foveolar metaplasia–hypermucinous dysplasia–mucinous adenocarcinoma sequence in IBD. Overall, this study extends international findings to a Central-Eastern European population and highlights the diagnostic and clinical significance of recognizing NCD in IBD-associated neoplasia.

2. This retrospective study from the University of Szeged examined neoplastic specimens from IBD patients to identify NCDs and evaluate their clinicopathological relevance. NCDs were most often associated with UC and found predominantly in the left colon, with serrated dysplasia, NOS and hypermucinous types being the most common. Their presence was linked to the development of CRC, and more advanced tumor stage. Unlike North American studies, certain NCD subtypes such as crypt cell and domed dysplasia were absent, indicating possible regional differences. Overall, this study highlights the importance of recognizing NCDs in IBD-related neoplasia and supports more vigilant endoscopic surveillance and complete lesion removal for affected patients.

3. This study highlights important advances in understanding serrated dysplastic lesions in IBD. The findings show that SSL-like dysplasia in IBD displays distinctive clinicopathologic and molecular profiles compared with its sporadic counterpart, including unique mutations not previously reported in serrated lesions. Notably, the discovery of *POLE*, *KMT2C*, and *EXT1* mutations suggests that these lesions may represent a novel molecular pathway and potential precursors to specific CRC subtypes. Serrated dysplasia, NOS, demonstrated distinct molecular alterations, such as *TP53* and *POLG* mutations, and appeared to carry a higher malignant potential. Overall, these achievements refine the molecular classification of IBD-associated serrated dysplasia and underscore the importance of complete excision.

7. ACKNOWLEDGEMENT

I am very grateful to my supervisor, Anita Sejben from the Department of Pathology at the University of Szeged, for her constant help, guidance, and her endless patience through my work.

I am grateful for all the coauthors I had the privilege of working with, including Won-Tak Choi, Georgios Deftereos, Bence Kővári, Tamás Lantos, Levente Kuthi, Szintia Almási, Bence Baráth, Panna Szaszák, Zsófia Krisztina Török.

I would like to thank the Albert Szent-Györgyi Medical School for supporting our research with the Géza Hetényi Fund (IV-134-62-1/2024.SZAOK).

I also thank the previously unlisted members of the multidisciplinary gastroteam of the University of Szeged, who helped me with my studies in general gastrointestinal clinicopathology.

Special thanks to all my coworkers at the Department of Pathology, University of Szeged. I am grateful to the doctors for helping me learn my field and to all our technicians, without whose high-quality work we would not be able to work or do research.

Naturally, the patients themselves merit recognition for contributing to the analyses of their disease and the potential benefit of the results to other patients.

I am very grateful for Roland Fejes, my loved ones and friends, without whom, this work could not have been completed.

8. REFERENCES

- [1] Pegagna L, Antonelli A, Ganini C, Bellato V, Campanelli M, Divizia A, Efrati C, Franceschilli M, Guida AM, Ingallinella S, Montagnese F, Sensi B, Siragusa L, Sica GS. Pathophysiology of Crohn's disease inflammation and recurrence. *Biol Direct* (2020) 15:23. doi:10.1186/s13062-020-00280-5
- [2] Nagao-Kitamoto H, Kitamoto S, Kamada N. Inflammatory bowel disease and carcinogenesis. *Cancer Metastasis Rev* (2022) 41:301–316. doi:10.1007/s10555-02210028-4
- [3] Satsangi J, Silverberg MS, Vermeire S, Colombel JF. The Montreal classification of inflammatory bowel disease: controversies, consensus and implications. *Gut* (2006) 55:749–753. doi:10.1136/gut.2005.082909
- [4] Shah SC, Itzkowitz SH. Colorectal cancer in inflammatory bowel disease: mechanisms and management. *Gastroenterology* (2022) 162:715–30.e3. doi:10.1053/j.gastro.2021.10.035
- [5] Alipour Z, Stashek K. Recently described types of dysplasia associated with IBD: tips and clues for the practising pathologist. *J Clin Pathol* (2024) 77:77–81. doi:10.1136/jcp-2023-209141
- [6] Choi WT. Non-conventional dysplastic subtypes in inflammatory bowel disease: a review of their diagnostic characteristics and potential clinical implications. *J Pathol Transl Med* (2021) 55:83–93. doi:10.4132/jptm.2021.02.17
- [7] Ungaro R, Colombel F, Lissos T, Peyrin-Biroulet L. A treat-to-target update in ulcerative colitis: a systematic review. *Am J Gastroenterol* (2019) 114:874–883. doi:10.14309/ajg.0000000000000183
- [8] Salla M, Guo J, Joshi H, Gordon M, Dooky H, Lai J, Capicio S, Armstrong H, Valcheva R, Dyck JRB, Thiesen A, Wine E, Dieleman LA, Baksh S. Novel biomarkers for inflammatory bowel disease and colorectal cancer: an interplay between metabolic dysregulation and excessive inflammation. *Int J Mol Sci* (2023) 24:5967. doi:10.3390/ijms24065967

- [9] Katsanos KH, Vermeire S, Christodoulou DK, Riis L, Wolters F, Odes S, Freitas J, Hoie O, Beltrami M, Fornaciari G, Clofent J, Bodini P, Vatn M, Borralho Nunes P, Moum B, Munkholm P, Limonard C, Stockbrugger R, Rutgeerts P, Tsianos EV; EC-IBD Study Group. Dysplasia and cancer in inflammatory bowel disease 10 years after diagnosis: results of a population-based European collaborative follow-up study. *Digestion* (2007) 75:113–121. doi:10.1159/000104731
- [10] Söderlund S, Brandt L, Lapidus A, Karlén P, Broström O, Löfberg R, Ekblom A, Askling J. Decreasing time-trends of colorectal cancer in a large cohort of patients with inflammatory bowel disease. *Gastroenterology* (2009) 136:1561–1819. doi:10.1053/j.gastro.2009.01.064
- [11] Almási Sz, Baráth B, Szaszák P, Kővári B, Sejben A. Hypermucinous and goblet cell deficient, IBD-associated, non-conventional dysplasia besides colorectal adenocarcinoma—case presentation. *Orv Hetil* (2023) 164:2039–2044. doi:10.1556/650.2023.32946
- [12] Riddell RH, Goldman H, Ransohoff DF, Appelman HD, Fenoglio CM, Haggitt RC, Ahren C, Correa P, Hamilton SR, Morson BC. Dysplasia in inflammatory bowel disease: standardized classification with provisional clinical applications. *Mod Pathol* (1983) 14:931–968. doi:10.1016/s0046-8177(83)80175-0
- [13] Choi WT, Yozu M, Miller GC, Shih AR, Kumarasinghe P, Misdraji J, Harpaz N, Lauwers GY. Nonconventional dysplasia in patients with inflammatory bowel disease and colorectal carcinoma: a multicenter clinicopathologic study. *Mod Pathol* (2020) 33:933–943. doi:10.1038/s41379-019-0419-1
- [14] Lee H, Rabinovitch PS, Mattis AN, Lauwers GY, Choi WT. Non-conventional dysplasia in inflammatory bowel disease is more frequently associated with advanced neoplasia and aneuploidy than conventional dysplasia. *Histopathology* (2021) 78:814–830. doi:10.1111/his.14298
- [15] Choi WT, Salomao M, Zhao L, Alpert L, Setia N, Liao X, Drage MG, Westerhoff M, Cheng J, Lauwers GY, Ko HM. Hypermucinous, goblet cell-deficient and crypt cell dysplasias in inflammatory bowel disease are often associated with flat/invisible endoscopic appearance

and advanced neoplasia on follow-up. *J Crohns Colitis* (2022) 16:98–108. doi:10.1093/ecco-jcc/jjab120

[16] Akarca FG, Yozu M, Alpert L, Kővári BP, Zhao L, Salomao M, Liao X, Westerhoff M, Lauwers GY, Choi WT. Non conventional dysplasia is frequently associated with low-grade tubuloglandular and mucinous adenocarcinomas in inflammatory bowel disease. *Histopathology* (2023) 83:276–285. doi:10.1111/his.14922

[17] Xiao A, Yozu M, Kővári BP, Yassan L, Salomao M, Westerhoff M, Sejben A, Lauwers GY, Choi WT. Nonconventional dysplasia is frequently associated with goblet cell deficient and serrated variants of colonic adenocarcinoma in inflammatory bowel disease. *Am J Surg Pathol* (2024) 48:691–698. doi:10.1097/PAS.0000000000002217

[18] Bahceci D, Sejben A, Yassan L, Miller G, Liao X, Ko HM, Salomao M, Yozu M, Lauwers GY, Choi WT. Inflammatory bowel disease-associated serrated lesions with dysplasia are frequently associated with advanced neoplasia: Supporting a unified classification approach. *Histopathology* (2025) 87:408-423. doi:10.1111/his.15448

[19] Ko HM, Harpaz N, McBride RB, Cui M, Ye F, Zhang D, Ullmann TA, Polydorides A. Serrated colorectal polyps in inflammatory bowel disease. *Mod Pathol* (2015) 28:1584–1593. doi:10.1038/modpathol.2015.111

[20] Miller GC, Liu C, Bettington ML, Leggett B, Whitehall VL, Rosty C. Traditional serrated adenoma-like lesions in patients with inflammatory bowel disease. *Hum Pathol* (2020) 97:19–28. doi:10.1016/j.humpath.2019.12.005

[21] DeJong ME, Nagtegaal ID, Vos S, van der Prost RS, van Herwaarden Y, Derikx LAAP, Hoentjen F. Increased colorectal neoplasia risk in patients with inflammatory bowel disease and serrated polyps with dysplasia. *Dig Dis Sci* (2022) 67:5647–5656. doi:10.1007/s10620-022-07485-w

[22] Nishio M, Kunisaki R, Shibata W, Ajioka Y, Hirasawa K, Takase A, Chiba S, Inayama Y, Ueda W, Okawa K, Otake H, Ogashiwa T, Kinoshita H, Saigusa Y, Kimura H, Kato J, Maeda

S. Serrated polyps in patients with ulcerative colitis: Unique clinicopathological and biological characteristics. *PLoS ONE* (2023) 18:e0282204. doi:10.1371/journal.pone.0282204

[23] Zhang R, Lauwers GY, Choi WT. Increased risk of non-conventional and invisible dysplasias in patients with primary sclerosing cholangitis and inflammatory bowel disease. *J Crohns Colitis* (2022) 16:1825–1834. doi:10.1093/ecco-jcc/jjac090

[24] Harpaz N, Goldblum JR, Shepherd NA, Riddell RH, Rubio CA, Vieth M, Wang HH, Odze RD. Colorectal dysplasia in chronic inflammatory bowel disease: a contemporary consensus classification and interobserver study. *Hum Pathol* (2023) 138:49–61. doi:10.1016/j.humpath.2023.05.008

[25] Choi WT. Characteristics, reporting, and potential clinical significance of nonconventional dysplasia in inflammatory bowel disease. *Surg Pathol Clin* (2023) 16:687–702. doi:10.1016/j.path.2023.05.006

[26] Choi WT, Kővári BP, Lauwers GY. The significance of flat/invisible dysplasia and nonconventional dysplastic subtypes in inflammatory bowel disease: a review of their morphologic, clinicopathologic, and molecular characteristics. *Adv Anat Pathol* (2022) 29:15–24. doi:10.1097/pap.0000000000000316

[27] Pereira D, Kővári B, Brown I, Chaves P, Choi WT, Clauditz T, Ghayouri M, Jiang K, Miller GC, Nakanishi Y, Kim KM, Kim BH, Kumarasinghe MP, Kushima R, Ushiku T, Yozu M, Srivastava A, Goldblum JR, Pai RK, Lauwers GY. Non conventional dysplasias of the tubular gut: a review and illustration of their histomorphological spectrum. *Histopathology* (2021) 78:658–675. doi:10.1111/his.14294

[28] OncoKB Database. Available online: <https://www.oncokb.org/> (accessed on 30 October 2025)

[29] ClinVar Database. Available online: <https://www.ncbi.nlm.nih.gov/clinvar/> (accessed on 30 October 2025)

- [30] Andersen SN, Lovig T, Clausen OP, Bakka A, Fausa O, Rognum TO. Villous, hypermucinous mucosa in long standing ulcerative colitis shows high frequency of K-ras mutations. *Gut* (1999) 45:686–692. doi:10.1136/gut.45.5.686
- [31] Patil DT, Goldblum JR, Odze RD. Immunohistochemical and molecular characterisation of dysplasia subtypes in ulcerative colitis. *Mod Pathol* (2017) 30:194A.
- [32] Nguyen ED, Wang D, Lauwers GY, Choi WT. Increased histologic inflammation is an independent risk factor for nonconventional dysplasia in ulcerative colitis. *Histopathology* (2022) 81:644–652. doi:10.1111/his.14765
- [33] Zhang R, Rabinovitch PS, Mattis AN, Lauwers GY, Choi WT. DNA content abnormality frequently develops in the right/proximal colon in patients with primary sclerosing cholangitis and inflammatory bowel disease and is highly predictive of subsequent detection of dysplasia. *Histopathology* (2023) 83: 116–125. doi:10.1111/his.14913
- [34] Lang-Schwarz C, Büttner-Herold M, Burian S, Erber R, Hartmann A, Jesinghaus M, Kamarádová K, Rubio CA, Seitz G, Sterlacci W, Vieth M, Bertz S. Morphological subtypes of colorectal low-grade intraepithelial neoplasia: diagnostic reproducibility, frequency and clinical impact. *J Clin Pathol* (2023) 209206–2023-209206. doi:10.1136/jcp-2023-209206
- [35] Nasreddin N, Jansen M, Loughrey MB, Wang LM, Koelzer VH, Rodriguez-Justo M, Novelli M, Fisher J, Brown MW, Al Bakir I, L Hart AL, Dunne P, Graham TA, Leedham SJ. Poor diagnostic reproducibility in the identification of nonconventional dysplasia in colitis impacts the application of histologic stratification tools. *Mod Pathol* (2023) 37:100419. doi:10.1016/j.modpat.2023.100419
- [36] Musulen E, Gené M, Cuatrecasas M, Amat I, Veiga JA, Fernández-Aceñero MJ, Chimisana VF, Tarragona J, Jurado I, Fernández-Victoria R, Martínez-Ciarpaglini C, González CA, Zac C, Fernández-Figueras MT, Esteller M. Gastric metaplasia as a precursor of nonconventional dysplasia in inflammatory bowel disease. *Hum Pathol* (2023) 143:50–61. doi:10.1016/j.humpath.2023.11.011

[37] Wen KW, Umetsu SE, Goldblum JR, Gill RM, Kim GE, Joseph NM, Rabinovitch PR, Kakar S, Lauwers GY, Choi WT. DNA flow cytometric and interobserver study of crypt cell atypia in inflammatory bowel disease. *Histopathology* (2019) 75:578–588. doi:10.1111/his.13923

[38] Kővári B, Clauditz T, Kamarádová K, Bathori A, Hegedus F, Miller G, Salomao M, Sejben A, Svrcek M, Yozu M, Kumarasinghe P, Pai R, Choi WT, Lauwers GY. Hypermucinous dysplasia in inflammatory bowel disease: a heterogeneous condition with frequent foveolar differentiation. *Mod Pathol* (2022) 35:481–482. doi:10.1038/s41379-022-01036-4

[39] Guerini C, Furlan D, Ferrario G, Grillo F, Libera L, Arpa G, Catherine Klersy C, Lenti MV, Riboni R, Solcia E, Fassan M, Mastracci L, Ardizzone S, Moens A, De Hertogh G, Ferrante M, Graham RP, Fausto Sessa F, Paulli M, Di Sabatino A, Vanoli A. IDH1 mutated Crohn's disease-associated small bowel adenocarcinomas: distinctive pathological features and association with MGMT methylation and serrated type dysplasia. *Histopathology* (2024) 84:515–524. doi:10.1111/his.15095

[40] Arpa G, Vanoli A, Grillo F, Fiocca R, Klersy C, Furlan D, Fausto Sessa F, Sandro Ardizzone S, Gianluca Sampietro G, Maria Cristina Macciomei MC, Gabriella Nesi G, Francesco Tonelli F, Carlo Capella C, Giovanni Latella G, Antonio Ciardi A, Caronna R, Lenti MV, Ciccocioppo R, Barresi V, Malvi D, D'Errico A, Rizzello F, Poggioli G, Mescoli C, Rugge M, Luinetti O, Paulli M, Di Sabatino A, Solcia E. Prognostic relevance and putative histogenetic role of cytokeratin 7 and MUC5AC expression in Crohn's disease-associated small bowel carcinoma. *Virchows Arch* (2021) 479:667–678. doi:10.1007/s00428-021-03109-2

[41] Kamarádová K. Non-conventional types of dysplastic changes in gastrointestinal tract mucosa- review of morphological features of individual subtypes. *Cesk Patol* (2022) 58:38–51.

[42] Waters KM, Singhi AD, Montgomery EA. Exploring the spectrum of serrated epithelium encountered in inflammatory bowel disease. *Hum Pathol* (2023) 132:126–134. doi:10.1016/j.humpath.2022.06.018

[43] Enea D, Lauwers G, Svrcek M. Dysplasies conventionnelles et non conventionnelles compliquant les maladies inflammatoires chroniques de l'intestin [Conventional and non-

conventional dysplasia in patients with inflammatory bowel disease]. *Ann Pathol* (2023) 43:180–191. doi:10.1016/j.annpat.2023.02.006

[44] Bahceci D, Lauwers GY, Choi WT. Clinicopathologic features of undetected dysplasia found in total colectomy or proctocolectomy specimens of patients with inflammatory bowel disease. *Histopathology* (2022) 81:183–191. doi:10.1111/his.14673

[45] Kamarádová K, Vošmíková H, Rozkošová K, Ryška A, Tachecí I, Laco J. Morphological, immunohistochemical and molecular features of inflammatory bowel disease associated colorectal carcinoma and associated mucosal lesions single institution experience. *Pathol Res Pract* (2019) 215:730–737. doi:10.1016/j.prp.2019.01.010

[46] Kamarádová K, Vošmíková H, Rozkošová K, Ryška A, Tachecí I, Laco J. Non conventional mucosal lesions (serrated epithelial change, villous hypermucinous change) are frequent in patients with inflammatory bowel disease-results of molecular and immunohistochemical single institutional study. *Virchows Arch* (2020) 476:231–241. doi:10.1007/s00428-019-02627-4

[47] Gutic B, Bozanovic T, Mandic A, Dugalic S, Todorovic J, Stanisavljevic D, Dugalic MG, Sengul D, Detanac DA, Sengul I, Detanac D, Soares Junior JM. Programmed cell death-1 and its ligands: current knowledge and possibilities in immunotherapy. *Clinics (Sao Paulo)* (2023) 78:100177. doi:10.1016/j.clinsp.2023.100177

[48] Gordon H, Biancone L, Fiorino G, Katsanos KH, Kopylov U, Al Sulais E, Axelrad JE, Balendran K, Burisch J, de Ridder L, Derikx L, Ellul P, Greuter T, Iacucci M, Di Jiang C, Kapizioni C, Karmiris K, Kirchgessner J, Laharie D, Lobatón T, Molnár T, Noor NM, Rao R, Saibeni S, Scharl M, Vavricka SR, Raine T. ECCOguidelines on inflammatory bowel disease and malignancies. *J Crohns Colitis* (2023) 17:827–854. doi:10.1093/ecco-jcc/jjac187

[49] Jung P, Kim HW, Park SB, Kang DH, Choi CW, Kim SJ, Nam HS, Ryu DG, Shin DH, Na JY, Yun MS. Clinical and endoscopic characteristics of sessile serrated lesions with dysplasia/carcinoma. *Korean J Intern Med* (2023) 38:349–361. doi:10.3904/kjim.2022.322

- [50] Cenaj O, Gibson J, Odze RD. Clinicopathologic and outcome study of sessile serrated adenomas/polyps with serrated versus intestinal dysplasia. *Mod Pathol* (2018) 31:633–642. doi:10.3904/kjim.2022.322
- [51] Bettington M, Walker N, Rosty C, Brown I, Clouston A, McKeone D, Pearson SA, Leggett B, Whitehall V. Clinicopathological and molecular features of sessile serrated adenomas with dysplasia or carcinoma. *Gut* (2017) 66:97–106. doi:10.1136/gutjnl-2015-310456
- [52] Liu C, Walker NI, Leggett BA, Whitehall VL, Bettington ML, Rosty C. Sessile serrated adenomas with dysplasia: Morphological patterns and correlations with MLH1 immunohistochemistry. *Mod Pathol* (2017) 30:1728–1738. doi:10.1038/modpathol.2017.92
- [53] Murakami T, Sakamoto N, Ritsuno H, Shibuya T, Osada T, Mitomi H, Yao T, Watanabe S. Distinct endoscopic characteristics of sessile serrated adenoma/polyp with and without dysplasia/carcinoma. *Gastrointest Endosc* (2017) 85:590–600. doi:10.1016/j.gie.2016.09.018
- [54] Lash RH, Genta RM, Schuler CM. Sessile serrated adenomas: Prevalence of dysplasia and carcinoma in 2139 patients. *J Clin Pathol* (2010) 63:681–686. doi:10.1136/jcp.2010.075507
- [55] Kawai T, Nyuya A, Mori Y, Tanaka T, Tanioka H, Yasui K, Toshima T, Taniguchi F, Shigeyashu K, Umeda Y, Fujiwara T, Okawaki M, Yamaguchi Y, Goel A, Nagasaka T. Clinical and epigenetic features of colorectal cancer patients with somatic POLE proofreading mutations. *Clin Epigenetics* (2021) 13:117. doi:10.1186/s13148-021-01104-7
- [56] Hu H, Cai W, Wu D, Hu W, Wang LD, Mao J, Zheng S, Ge W. Ultra-mutated colorectal cancer patients with POLE driver mutations exhibit distinct clinical patterns. *Cancer Med* (2021) 10:135–142. doi:10.1002/cam4.3579
- [57] Ahn SM, Ansari AA, Kim J, Kim D, Chun SM, Kim J, Kim TW, Park I, Yu CS, Jang SJ. The somatic POLE P286R mutation defines a unique subclass of colorectal cancer featuring hypermutation, representing a potential genomic biomarker for immunotherapy. *Oncotarget* (2016) 7:68638–68649. doi:10.18632/oncotarget.11862

- [58] Pancsa T, Vasas B, Meleg Z, Tóth E, Torday L, Sejben A. POLE-mutant colon adenocarcinoma-case presentation and histopathological evaluation. *J Gastrointest Cancer* (2024) 55:961–964. doi:10.1007/s12029-023-01004-4
- [59] Puccini A, Lenz HJ, Marshall JL, Arguello D, Raghavan D, Korn WM, Weinberg WA, Poorman K, Heeke AL, Philip PA, Shields AF, Goldberg RM, Salem ME. Impact of patient age on molecular alterations of left-sided colorectal tumors. *Oncologist* (2019) 24:319–326. doi:10.1634/theoncologist.2018-0117
- [60] Tanteles GA, Nicolaou M, Neocleous V, Shammash C, Loizidou MA, Alexandrou A, Ellina E, Patsia N, Sismani C, Phylactou LA, Christophidou-Anastasiadou V. Genetic screening of EXT1 and EXT2 in Cypriot families with hereditary multiple osteochondromas. *J Genet* (2015) 94:749–754. doi:10.1007/s12041-015-0564-3
- [61] Murakami T, Akazawa Y, Yatagai N, Hiromoto T, Sasahara N, Saito T, Sakamoto N, Nagahara A, Yao T. Molecular characterization of sessile serrated adenoma/polyps with dysplasia/carcinoma based on immunohistochemistry, next-generation sequencing, and microsatellite instability testing: A case series study. *Diagn Pathol* (2018) 13:88. doi:10.1186/s13000-018-0771-3
- [62] Day FL, Jorissen RN, Lipton L, Mouradov D, Shakhthianandeswaren A, Christie M, Li S, Tsui C, Tie J, Deasi J, Xu Z, Molloy P, Whitehall V, Leggett BA, Jones IT, McLaughlin S, Ward RL, Hawkins NJ, Ruzsiewicz AR, Moore J, Busam D, Zhao Q, Strausberg RL, Gibbs P, Sieber OM. PIK3CA and PTEN gene and exon mutation-specific clinicopathologic and molecular associations in colorectal cancer. *Clin Cancer Res* (2013) 19:3285–3296. doi:10.1158/1078-0432.CCR-12-3614
- [63] Lang-Schwarz C, Büttner-Herold M, Burian S, Erber R, Hartmann A, Jesinghaus M, Kamarádová K, Rubio CA, Seitz G, Sterlacci W, Vieth M, Bertz M. Morphological subtypes of colorectal low-grade intraepithelial neoplasia: Diagnostic reproducibility, frequency and clinical impact. *J Clin Pathol* (2025) 78:103–110. doi:10.1136/jcp-2023-209206

- [64] Samowitz WS, Sweeney C, Herrick J, Albertsen H, Levin TR, Murtaugh MA, Wolff RK, Slattery ML. Poor survival associated with the BRAF V600E mutation in microsatellite-stable colon cancers. *Cancer Res* (2005) 65:6063–6069. doi:10.1158/0008-5472.CAN-05-0404
- [65] Pai RK, Jayachandran P, Koong AC, Chang DT, Kwok S, Ma L, Arber DA, Balise RR, Tubbs RR, Shadrach B, Pai RK. BRAF-mutated, microsatellite-stable adenocarcinoma of the proximal colon: An aggressive adenocarcinoma with poor survival, mucinous differentiation, and adverse morphologic features. *Am J Surg Pathol* (2012) 36:744–752. doi:10.1097/PAS.0b013e31824430d7
- [66] Bond CE, Umapathy A, Ramsnes I, Greco SA, Zhao ZZ, Mallitt KA, Buttenshaw RL, Montgomery GW, Leggett BA, Whitehall VLJ. P53 mutation is common in microsatellite stable, BRAF mutant colorectal cancers. *Int J Cancer* (2012) 130:1567–1576. doi:10.1002/ijc.26175
- [67] Linkowska K, Jawie'n A, Marszałek A, Malyarchuk BA, To'nska K, Bartnik E, Skonieczna K, Grzybowski T. Mitochondrial DNA polymerase γ mutations and their implications in mtDNA alterations in colorectal cancer. *Ann Hum Genet* (2015) 79:320–328. doi:10.1111/ahg.12111
- [68] Maiuri AR, Li H, Stein BD, Tennessen JM, O'Hagan HM. Inflammation-induced DNA methylation of DNA polymerase gamma alters the metabolic profile of colon tumors. *Cancer Metab* (2018) 6:9. doi:10.1186/s40170-018-0182-7